AD_____

Award Number: DAMD17-00-1-0345

TITLE: Genetic Determinants of Inflammatory Breast Cancer

PRINCIPAL INVESTIGATOR: Sofia Merajver

CONTRACTING ORGANIZATION: University of Michigan
Ann Arbor, Michigan 48109-1274

REPORT DATE: July 2001

TYPE OF REPORT: Annual

PREPARED FOR: U.S. Army Medical Research and Materiel Command
Fort Detrick, Maryland 21702-5012

REPORT DOCUMENTATION PAGE

Form Approved
OMB No. 074-0188

1. AGENCY USE ONLY (Leave blank)	2. REPORT DATE	3. REPORT TYPE AND DATES COVERED
	July 2001	Annual (15 Jun 00 - 14 Jun 01)

4. TITLE AND SUBTITLE
Genetic Determinants of Inflammatory Breast Cancer

5. FUNDING NUMBERS
DAMD17-00-1-0345

6. AUTHOR(S)
Sofia Merajver

7. PERFORMING ORGANIZATION NAME(S) AND ADDRESS(ES)
University of Michigan
Ann Arbor, Michigan 48109-1274

E-Mail: smerajve@umich.edu

8. PERFORMING ORGANIZATION REPORT NUMBER

9. SPONSORING / MONITORING AGENCY NAME(S) AND ADDRESS(ES)
U.S. Army Medical Research and Materiel Command
Fort Detrick, Maryland 21702-5012

10. SPONSORING / MONITORING AGENCY REPORT NUMBER

11. SUPPLEMENTARY NOTES

12a. DISTRIBUTION / AVAILABILITY STATEMENT
Approved for Public Release; Distribution Unlimited

12b. DISTRIBUTION CODE

13. ABSTRACT *(Maximum 200 Words)*

Primary inflammatory breast cancer (IBC) accounts for approximately 6% of new breast cancers annually. We hypothesized that a limited number of concordant genetic alterations give rise to the unique aggressive inflammatory phenotype of IBC. While working on the genetic determinants underlying the IBC phenotype, we found concordant and consistent alterations of two genes, RhoC GTPase and a novel IGF-binding protein (IGF-BP), in patients with IBC. RhoC was overexpressed in 90% of IBC samples examined compared to 30% of stage matched non-IBC tumors. LIBC was lost in 80% of the IBC samples and only 20% of the non-IBC samples examined. Since RhoC and LIBC appear to act in concert in IBC, coupled to the preliminary evidence from other laboratories of genes from these families playing a role in pancreatic cancer (another highly aggressive adenocarcinoma), they are excellent candidate genes to begin to probe the genetic basis of the aggressive phenotype in IBC. We hypothesize that the phenotype of IBC is due to alterations in expression of RhoC and IGF-BP early in tumorigenesis. We will elucidate the signaling pathway downstream from RhoC GTPase and attempt to determine what effect RhoC and LIBC have on cellular motility and invasion.

14. SUBJECT TERMS
Motility, invasion, aggressive phenotype

15. NUMBER OF PAGES
111

16. PRICE CODE

17. SECURITY CLASSIFICATION OF REPORT	18. SECURITY CLASSIFICATION OF THIS PAGE	19. SECURITY CLASSIFICATION OF ABSTRACT	20. LIMITATION OF ABSTRACT
Unclassified	Unclassified	Unclassified	Unlimited

Table of Contents

Sofia D. Merajver, M.D., Ph.D.
Annual Report for Award Number: DAMD17-00-1-0345
August 21, 2001

Introduction:

This is a progress report for a project that aims at understanding the genetic determinants of Inflammatory Breast Cancer (IBC). In particular, we aim to discern the relative role of the RhoC GTPase gene as well as a gene named WISP3 (formally LIBC) in the specific phenotypic characteristics of Inflammatory Breast Cancer. We have made significant progress in the last year which is summarized below.

Body:

The major thrust of our year's work has been in understanding the functional significance of the WISP3 gene in Inflammatory Breast Cancer. An accompanying manuscript is now under review. Likewise, we have published one report dealing with the expression of E-Cadherin in Inflammatory Breast Cancer. Interestingly, our laboratory group was able to define the surprising finding that E-Cadherin expression is preserved as Inflammatory Breast Cancer cells as they enter into the dermal lymphatics; this is not completely unexpected but somewhat of a surprising finding given that, in general, E-Cadherin expression is associated with a lower metastatic potential. This is probably an erroneous generalization and it does not apply to the case of Inflammatory Breast Cancer, where the establishment of clumps of tumor cells that plug the dermal lymphatics appears to require E-Cadherin expression. Another aspect of our work has been on understanding RhoC signaling and how RhoC elicits motility and angiogenesis and an attached manuscript has been prepared as a report and is now submitted. We have found that the MAP kinase and p38 pathways contribute differentially to motility and angiogenesis in Inflammatory Breast Cancer mediated by RhoC.

We have completed a study on the effect of farnesyl transferase inhibitors on RhoC manuscript detailing these findings is nearing completion.

In summary, we have had a very productive year where we have completed several manuscripts dealing with key aspects of the regulation of RhoC expression in Inflammatory Breast Cancer phenotypes and also the phenotypic effects of RhoC overexpression. In addition, we have completed a major effort in understanding the function of the WISP3 gene as it contributes to the phenotype in Inflammatory Breast Cancer.

Key Research Accomplishments:

The key research accomplishments are summarized above and the following is a list of new manuscripts and abstracts either published or under review during the last year. We now understand how RhoC signals inside the cell to elicit motility and angiogenesis. We have made significant progress in our understanding of how WISP3 elicits its function in breast cancer.

Reportable Outcomes:

We are in a position to definitively state that the angiogenic and motility characteristics of Inflammatory Breast Cancer are to a great extent due to the RhoC GTPase overexpression. In addition, we are able to definitively state that farnesyl transferase inhibitors should have activity against RhoC mediated phenotypes in breast cancer. We are working on defining the reportable outcome of the effect of RhoC overexpression and prognosis in early stage lesions, but that work is still ongoing.

Conclusion:

We are encouraged by our progress so far and continue to proceed with more specific functional studies of the signaling pathways that WISP3 is involved in. In particular, we wish to establish the relationship between WISP3 and ß-catenin in the development of resistance to apoptosis in cancer cells. We will report on those findings in next year's annual report.

References:

1. Kleer CG, van Golen KL, Braun T, Merajver SD: Persistent E-Cadherin Expression in Inflammatory Breast Cancer. *Mod Pathol* 14(5):458-464, 2001.

2. van Golen KL, Bao LW, Pan Q, Miller FR, Wu ZF, Merajver SD: Mitogen activated protein kinase pathway is involved in RhoC GTPase induced motility, invasion and angiogenesis in inflammatory breast cancer. *Clin Exp Metastasis* (submitted), 2001.

3. Kleer CG, Zhang Y, Pan Q, van Golen KL, Wu ZF, Livant D, Merajver SD: WISP3 Is a Novel Angiogenesis Inhibitor and Tumor Suppressor Gene of Inflammatory Breast Cancer. *J Clin Invest* (submitted), 2001.

4. Kleer CG, van Golen KL, Zhang Y, Wu ZF, Rubin MA, Merajver SD: Characterization of RhoC Expression in Benign and Malignant Breast Disease: A Potential New Marker for Small Breast Carcinomas with Metastatic Potential. *Am J Pathol* (submitted), 2001.

Persistent E-Cadherin Expression in Inflammatory Breast Cancer

Celina G. Kleer, M.D., Kenneth L. van Golen, Ph.D., Thomas Braun, Ph.D., Sofia D. Merajver, M.D., Ph.D.

Departments of Pathology (CGK), Internal Medicine, Division of Hematology and Oncology (KvG, SDM), and the University of Michigan Comprehensive Cancer Center (CGK, KvG, SDM, TB), Ann Arbor, Michigan

E-cadherin is a transmembrane glycoprotein that mediates epithelial cell-to-cell adhesion. Because loss of E-cadherin expression results in disruption of cellular clusters, it has been postulated that E-cadherin functions as a tumor suppressor protein. The role of E-cadherin in inflammatory breast cancer (IBC), a distinct and highly aggressive form of breast cancer, is largely unknown. The aim of our study was to elucidate whether E-cadherin expression contributes to the development and progression of the IBC phenotype and to investigate any differences in E-cadherin expression between IBC and stage-matched non-IBC. Forty-two breast cancer cases (20 IBC and 22 non-IBC) were identified. Strict and well-accepted criteria were used for the diagnosis of IBC. Clinical and pathologic features were studied, and formalin-fixed, paraffin-embedded tissue sections were immunostained for E-cadherin, estrogen and progesterone receptors (ER and PR, respectively), and HER2/*neu*. Statistical analysis was performed using Fisher's exact test. All IBC uniformly expressed E-cadherin, whereas 15 of the 22 (68%) of the non-IBC expressed the protein ($P = .006$). Intralymphatic tumor emboli in the IBC cases were also all E-cadherin positive. Two IBC tumors demonstrated invasive lobular histology, and both cases were positive for E-cadherin. Of the non-IBC cases, three were invasive lobular carcinomas, and all were positive for E-cadherin. No association was found between E-cadherin expression and ER, PR status, or HER2/neu overexpression. Our study demonstrates that there is a strong association between E-cadherin expression and IBC and suggests that E-cadherin may be involved in the pathogenesis of this form of advanced breast cancer. In our study, we demonstrate that circulating IBC tumor cells strongly express E-cadherin, thereby providing an important exception to the positive association between E-cadherin loss and poor prognosis in breast cancer.

KEY WORDS: Breast cancer, E-cadherin, Inflammatory breast cancer, Metastasis, Tumor emboli.

Mod Pathol 2001;14(5):458–464

Inflammatory breast cancer (IBC) accounts for approximately 6% of new breast cancers in the United States annually. It is the most aggressive and lethal form of locally advanced breast cancer, with a mean 5-year disease-free survival rate of <45% (1–3). IBC has unique clinical and pathological features. Clinically, patients present with skin erythema and nodularity; pathologically, IBC is highly angiogenic and angioinvasive, with numerous tumor emboli filling the dermal lymphatics. These tumor emboli are responsible for the striking clinical picture that arises from lymphatic obstruction (4–6).

E-cadherin is a transmembrane glycoprotein that mediates calcium-dependent intercellular adhesion and is specifically involved in epithelial cell-to-cell adhesion (7). Diminished E-cadherin expression has been related to the acquisition of invasiveness in experimental tumors and in advanced-stage carcinomas, including ductal carcinomas of the breast (7–12). Several studies have shown that E-cadherin expression is significantly reduced in high-grade, estrogen receptor (ER)–negative, and metastatic breast carcinomas (10, 13, 14). Loss of E-cadherin expression tends to appear in a heterogeneous pattern within carcinomas, suggesting that loss of expression of E-cadherin in these tumors is a potentially reversible somatic alteration. It is not known to what level circulating malignant cells with metastatic potential express E-cadherin.

A recent study reported overexpression of E-cadherin in IBC both in human and in an IBC xenograft model in SCID/nude mice (15). Given the unique highly metastatic IBC phenotype, we hy-

VOL. 14, NO. 5, P. 458, 2001 Printed in the U.S.A.

Date of acceptance: December 19, 2000.

Address reprint requests to: Celina G. Kleer, M.D., Department of Pathology, 2G332 University Hospital, 1500 E. Medical Center Drive, Ann Arbor, MI 48109-0054; e-mail: kleer@umich.edu; fax: 734-936-6776.

pothesized that IBC would exhibit a pattern of E-cadherin expression distinct from stage matched non-IBC. In addition, the high propensity of IBC cells to invade lymphatic channels makes IBC an interesting model to study E-cadherin expression in metastasis-enabled circulating cancer cells.

MATERIALS AND METHODS

Patient Selection

IBC and non-IBC patients were chosen using the computerized clinical database and by prospective identification of newly diagnosed patients. We identified 20 cases of IBC and 22 cases of stage-matched (Stages III and IV) non-IBC. All cases were obtained from the pathology files in our institution, and hematoxylin and eosin–stained slides were available for review in all cases. Strict and well-accepted criteria were used to make the diagnosis of IBC (4–6). Clinically, erythema over at least one third of the breast was required, with the classical peau d'orange appearance that includes skin thickening and erythema, with or without nodularity. Although the diagnosis of IBC is primarily clinical, all the IBC cases also had pathologically demonstrable tumor emboli in the dermal lymphatic channels. The non-IBC tumors presented as either palpable masses or mammographic abnormalities without skin changes, and pathologically, none of these cases contained dermal lymphatic tumor emboli, as assessed in nipple sections of the mastectomy specimens.

Immunohistochemistry

E-cadherin protein expression was studied by immunohistochemistry using specific monoclonal antibodies (Zymed Laboratories, San Francisco, CA). For assessment of ER, progesterone receptor (PR), and HER2/*neu* expression, specific monoclonal antibodies for ER (Ventana Medical Systems, Tucson, AZ), PR (DAKO, Carpinteria, CA), and HER2/neu (Herceptest from DAKO) were used at their manufacturers' recommended dilutions. Immunohistochemistry was performed as previously described using an automated immunostainer (Biotek Techmate 500, Ventana Medical Systems; 16). Briefly, 5-μm-thick sections were cut onto glass slides from formalin-fixed paraffin blocks. Sections were deparaffinized, microwaved (1000-watt Model MTC1080-2A; Frigidaire, Dublin, OH) in a pressure cooker (Nordic Ware, Minneapolis, MN) with 1 L 10 mM citrate buffer, pH 6.0. They were subsequently cooled with the lid on for an additional 10 minutes. After removing the lid, the entire pressure cooker was filled with cold running tap water for 2 to 3 minutes or until the slides were cool. At 36°C, the stainer sequentially added an inhibitor of endogenous peroxidase, the primary antibodies (32 minutes), a biotinylated secondary antibody, an avidin-biotin-complex with horseradish peroxidase, 3,3'-diaminobenzidine (3,3'-diaminobenzidine tetrahydrochloride), and copper enhancer. The slides were then counterstained with hematoxylin.

E-cadherin expression was interpreted as either positive or negative. To qualify as positive, complete and crisp membranous staining was required in ≥10% of the tumor cells. In the negative cases, internal positive controls, such as epidermis, lymphocytes, and benign breast lobules, were examined. ER and PR were considered positive when >5% of the tumor cell nuclei were stained. For HER2/*neu*, the strength of the membranous staining was recorded as 0 or as 1+ through 4+, and a sample was considered positive when ≥10% neoplastic cells had a staining intensity of 2+ or greater.

Statistical Analysis

Differences in percentages of E-cadherin positive cases between the IBC and non-IBC groups were tested for statistical significance using Fisher's exact test. A P value of ≤.05 was considered significant. A two-sample t test was also performed to compare the ages at diagnosis of the two groups of patients. Logistic regression was used to examine differences in E-cadherin expression between IBC and non-IBC patients, adjusted for age, ER and PR expression, and HER2/*neu* overexpression.

RESULTS

Clinical and Pathological Features

All patients were female. IBC patients ranged in age at diagnosis from 35 to 72 years (mean age, 51), and non-IBC patients ranged in age from 31 to 78 years (mean age, 59l). Twenty cases were diagnosed as IBC, and 22 cases as non-IBC. Thirty-four tumors (81%) were invasive ductal carcinomas (18 IBC, 16 non-IBC), five tumors (12%) were invasive lobular carcinomas (2 IBC, 3 non-IBC), one tumor was a medullary carcinoma (non-IBC), and another was an atypical medullary carcinoma (non-IBC). One tumor was an anaplastic carcinoma (non-IBC). There were no statistically significant differences in the frequency distribution of histologic tumor types between IBC and non-IBC tumors.

E-Cadherin Expression in IBC and Non-IBC Tumors and Its Relationship to ER, PR, HER2/*neu* Expression, and Angiolymphatic Invasion

All IBC strongly expressed E-cadherin, characterized by crisp staining of cell membranes in ≥10% of

the cells with a staining intensity of 2+ or more. Of note, the endolymphatic tumor emboli were also strongly positive for E-cadherin in all cases (Fig. 1). Of the 22 non-IBC tumors, 15 (68%) expressed E-cadherin and 7 (32%) cases did not. Table 1 shows the frequency of E-cadherin expression in IBC *versus* non-IBC. The difference in E-cadherin expression rates in IBC *versus* non-IBC was statistically significant ($P < .006$; Fig. 2). To exclude the possibility that the significant difference in E-cadherin expression between IBC and non-IBC tumors was influenced by age, ER, PR, and HER2/

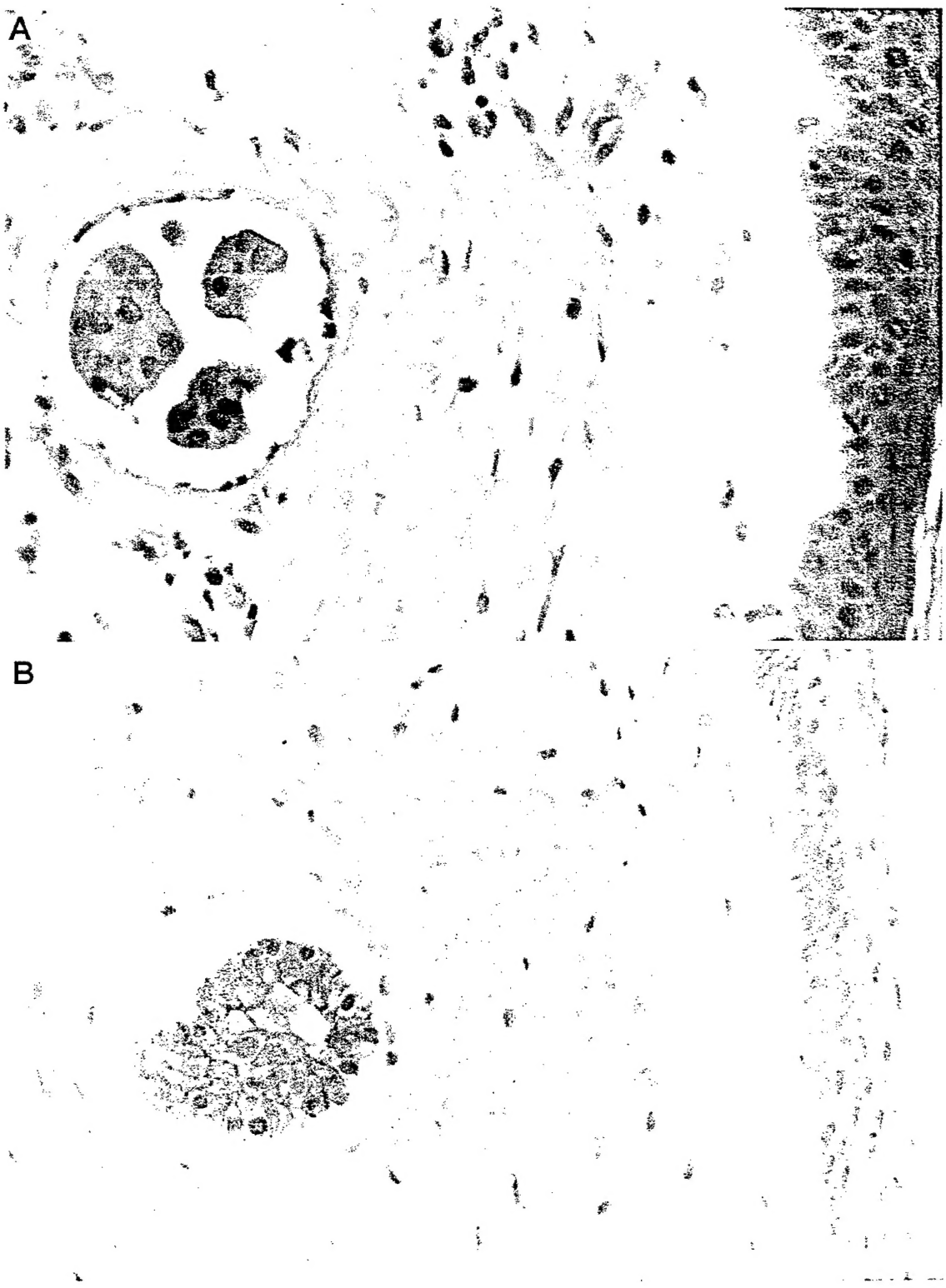

FIGURE 1. Inflammatory breast cancer with a characteristic tumor embolus in a dermal lymphatic channel (**A**) and strong and crisp membranous staining for E-cadherin in the intralymphatic tumor cells (**B**). Magnification: ×20.

TABLE 1. Relationship between E-Cadherin Expression, ER, PR, and HER2/*neu* Status in IBC *versus* Non-IBC Patients

	IBC: # of Positive Cases (%)	Non-IBC: # of Positive Cases (%)	*P* Value
E-cadherin expression	20 (100)	15 (68)	=.006
ER expression	7 (41)	8 (38)	>.05
PR expression	6 (35)	9 (43)	>.05
HER2/*neu* overexpression	5 (56)	6 (43)	>.05

ER, estrogen receptor; PR, progesterone receptors; IBC, inflammatory breast cancer; non-IBC, non–inflammatory breast cancer.

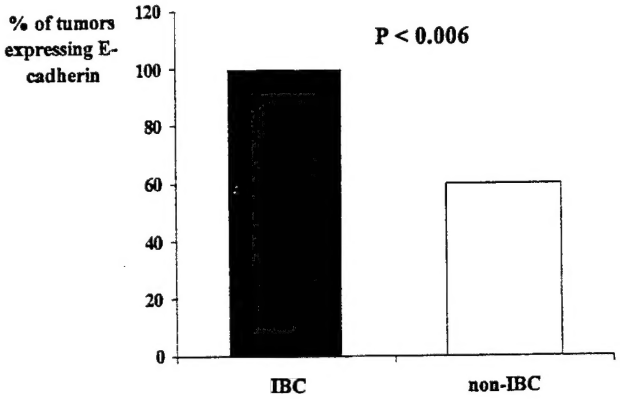

FIGURE 2. Analysis of E-cadherin expression in inflammatory breast cancer (IBC) *versus* non-IBC. The bars illustrate the statistically significant difference in E-cadherin expression between the two groups of tumors.

neu status, we used logistic regression after adjusting for these variables. The increased expression of E-cadherin in patients with IBC, as compared with non-IBC patients, remained statistically significant after adjustment. Interestingly, the two IBC with features of invasive lobular carcinomas expressed E-cadherin, in contrast to the three cases of invasive lobular carcinoma in the non-IBC group, which were all negative for E-cadherin (Fig. 3).

Of the 22 stage-matched, non-IBC tumors, 17 (77%) had angiolymphatic invasion and/or lymph node or distant metastases, and 5 tumors (23%) did not. E-cadherin was expressed in 11 (65%) and in 4 (80%) of the non-IBC with and without angiolymphatic invasion and/or metastases, respectively ($P < .005$). Thus, we observed a significant relationship between loss of E-cadherin expression and angiolymphatic invasion for non-IBC tumors.

Among the IBC tumors, seven cases (41%) were ER positive, and six cases (35%) were PR positive, equivalent to the non-IBC distribution, in which eight tumors (38%) expressed ER and nine tumors (43%) expressed PR. HER2/neu was overexpressed in five (56%) IBC tumors and in six (43%) of non-IBC tumors. Table 1 shows the relationship between E-cadherin expression, ER/PR status, and HER2/*neu* overexpression. No statistically significant differences in ER, PR, or HER2/*neu* status were observed between IBC and non-IBC tumors.

DISCUSSION

IBC is a very distinct form of breast carcinoma with unique clinical and pathologic features that pursues an extremely aggressive course (3, 4, 6). Because of these unique characteristics, we hypothesized that distinct genetic alterations may define the inflammatory phenotype. The present study provides a new insight into the E-cadherin–mediated cell-to-cell adhesion in the pathogenesis and/or progression of IBC as it demonstrates that E-cadherin is expressed in 100% of IBC and is preferentially expressed in IBC when compared to stage matched non-IBC.

The results of our study agree with a recent report by Alpaugh *et al.* (15), who developed a human xenograft model of IBC in SCID/nude mice that closely recapitulates the pathology of IBC in humans. These investigators detected by Western blot analysis 10- to 20-fold overexpression of E-cadherin in the xenografts and confirmed E-cadherin overexpression by immunohistochemistry in the xenografts and in cases of human IBC.

Compelling evidence exists in the literature to indicate that down-regulation of E-cadherin expression and/or function is a critical factor in the malignant progression of epithelial tumors (8, 11, 12). Transfection of E-cadherin into invasive carcinoma cell lines reduced their ability to invade *in vitro*, further supporting the role of E-cadherin in maintaining cells in an epithelial ordered state and suppressing the invasive potential of nascent malignant cells (11, 12). Furthermore, restoration of E-cadherin expression, initially lost in the transition from adenoma to invasive carcinoma, resulted in tumor arrest at the adenoma stage in a transgenic mouse model of pancreatic B-cell carcinogenesis (8). E-cadherin is thought to act as a tumor suppressor gene in the breast, although the mechanism of E-cadherin–mediated tumor suppression has not been fully elucidated (17). Previous reports showed low expression of E-cadherin in breast cancers with increased invasiveness and high metastatic potential (13, 14). Our results are in agreement with the literature in the sense that the non-IBC tumors with angiolymphatic invasion and/or metastases had significantly less E-cadherin expression than the tumors that did not have these features. Most important, we demonstrate that in IBC, the most aggressive form of breast cancer, 100% of cases show E-cadherin protein expression, regardless of the histologic type of the tumor or of ER, PR, or HER2/*neu* expression. It is very likely that previous studies comprised highly heterogeneous groups of tumors

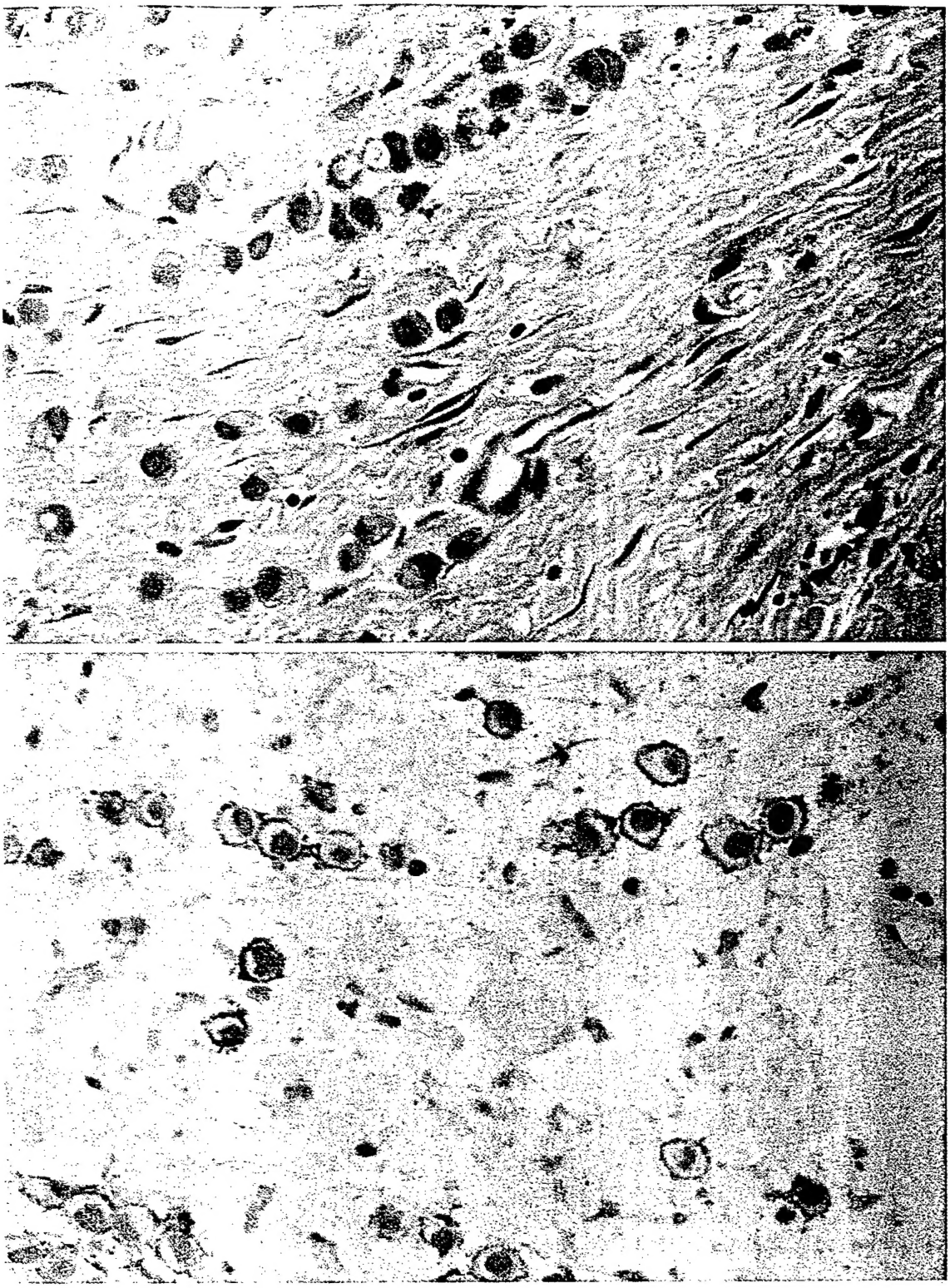

FIGURE 3. Primary inflammatory breast cancer with classic invasive lobular carcinoma histology, composed of files of small malignant cells, some of which have signet-ring cell features (A). Positive E-cadherin staining in the malignant cells with classic lobular morphology (B). The membranous staining highlights the signet-ring cell features of some of the neoplastic cells. Magnification: ×40.

in which very few cases would have been IBC. Our results indicate that E-cadherin does not appear to function as a tumor suppressor gene in IBC, and they are in support of recent studies that suggest a role for E-cadherin in cellular differentiation and survival (18–21). The different potential roles of E-cadherin in the pathogenesis of IBC and non-IBC warrant further investigation.

To metastasize, cancer cells must break away from the primary tumor, move into the surrounding

stroma, intravasate into the lymphatic or vascular circulation, extravasate, and successfully reestablish growth at other sites. Although it has long been postulated that in the course of metastasis development cancer cells lose E-cadherin expression and thereby intercellular adhesion, *in vivo* and *in vitro* studies have failed to correlate reduced E-cadherin expression with an invasive and metastatic phenotype (10, 22). Moreover, it is unknown whether E-cadherin expression is reduced in circulating cells before extravasation. In the present study, intralymphatic tumor cells strongly express E-cadherin, which challenges the hypothesis that loss of expression is a necessary event in the circulating cancer cells as they become metastasis enabled. On the basis of our results and the results of other investigations (23, 24), we suggest that loss of E-cadherin expression is a transient phenomenon that has the purpose of allowing malignant cells to invade vascular channels and tissues; we further suggest that once in the circulation, these cancer cells reinstate the expression of E-cadherin, facilitating intercellular adhesion and enabling the formation of cohesive tumor emboli. Interestingly, when analyzing E-cadherin expression at the primary site of non-IBC tumors, we found a highly significant correlation between loss of E-cadherin expression and presence of angiolymphatic invasion. This is consistent with other observations indicating that in non-IBC, loss of E-cadherin is a poor prognostic marker.

In breast cancer, reduced expression of E-cadherin has been reported in approximately 50% of invasive ductal carcinomas, whereas invasive lobular carcinomas showed complete loss of E-cadherin expression in nearly 90% of cases (17, 24, 25). Truncating E-cadherin mutations have been found in two thirds of invasive lobular carcinomas but in no invasive ductal carcinomas (26, 27). These studies suggest a relationship between loss of E-cadherin–mediated cell adhesion and the diffuse and discohesive pattern of growth that is characteristic of invasive lobular carcinoma. In the present study, two E-cadherin–positive IBC were histologically classic invasive lobular carcinomas. Of the non-IBC, three cases were invasive lobular carcinomas, all of which were E-cadherin negative. Despite the fact that the small number of cases precludes drawing firm conclusions on the possible relationship between the IBC phenotype, invasive lobular carcinoma histology, and E-cadherin expression, our results suggest that E-cadherin expression may have an even stronger positive association with the IBC phenotype than loss of E-cadherin expression does with the lobular morphology.

In conclusion, our study demonstrates a strong positive association between E-cadherin expression and the IBC phenotype. We further demonstrate that circulating tumor cells of IBC patients strongly express E-cadherin and that thus, IBC constitutes an important exception to the association between loss of E-cadherin expression and increased metastatic potential and poor outcome in breast cancer.

REFERENCES

1. Piera JM, Alonso MC, Ojeda MB, Biete A. Locally advanced breast cancer with inflammatory component: A clinical entity with a poor prognosis. Radiother Oncol 1986;7:199–204.
2. Stocks LH, Patterson FM. Inflammatory carcinoma of the breast. Surg Gynecol Obstet 1976;143:885–9.
3. Merajver SD, Weber BL, Cody R, Zhang D, Strawderman M, Calzone KA, *et al.* Breast conservation and prolonged chemotherapy for locally advanced breast cancer: The University of Michigan experience. J Clin Oncol 1997;15:2873–81.
4. Lee BJ, Tannenbaum NE. Inflammatory carcinoma of the breast: A report of twenty-eight cases from the breast clinic of Memorial Hospital. Surg Gynecol Obstet 1924;39:580–95.
5. Rosen PP. Rosen's breast pathology. Philadelphia: Lippincott-Raven; 1996.
6. Jaiyesimi I, Buzdar A, Hortobagyi G. Inflammatory breast cancer: A review. J Clin Oncol 1992;10:1014–24.
7. Takeichi M. Cadherin cell adhesion receptors as a morphogenetic regulator. Science 1991;51:1451–5.
8. Perl AK, Wilgenbus P, Dahl U, Semb H, Christofori G. A causal role for E-cadherin in the transition from adenoma to carcinoma. Nature 1998;392:190–3.
9. Christofori G, Semb H. The role of the cell-adhesion molecule E-cadherin as a tumour-suppressor gene. Trends Biochem Sci 1999;24:73–6.
10. Bukholm IK, Nesland JM, Karesen R, Jacobsen U, Borresen-Dale AL. E-cadherin and a-, β- and γ-catenin protein expression in relation to metastasis in human breast carcinoma. J Pathol 1998;3:262–6.
11. Frixen UH, Behrens J, Sachs M, Eberle G, Voss B, Warda A, *et al.* E-cadherin-mediated cell–cell adhesion prevents invasiveness of human carcinoma cells. J Cell Biol 1991;113:173–85.
12. Vleminckx K, Vakaet L Jr, Mareel M, Fiers W, van Roy F. Genetic manipulation of E-cadherin expression by epithelial tumor cells reveals an invasion suppressor role. Cell 1991; 66:107–19.
13. Siitonen SM, Kononen JT, Helin HJ, Rantala IS, Holli KA, Isola JJ. Reduced E-cadherin expression is associated with invasiveness and unfavorable prognosis in breast cancer. Am J Clin Pathol 1996;105:394–402.
14. Hunt NCA, Douglas-Jones AG, Jasani B, Morgan JM, Pignatelli M. Loss of E-cadherin expression associated with lymph node metastases in small breast carcinomas. Virchows Arch 1997;430:285–9.
15. Alpaugh ML, Tomlinson JS, Shao ZM, Barsky SH. A novel human xenograft model of inflammatory breast cancer. Cancer Res 1999;59:5079–84.
16. Kleer CG, Wojno KJ, Fields K, Singleton TP. Detection of estrogen receptor in carcinomas of the breast using automated immunohistochemistry. Appl Immunohistochem Mol Morphol 1999;7:103–7.
17. Peralta Soler A, Knudsen KA, Jaurand MC, Johnson KR, Wheelock MJ, Klein-Szanto AJ, *et al.* The differential expression of N-cadherin and E-cadherin distinguishes pleural mesotheliomas from lung adenocarcinomas. Hum Pathol 1995; 26:1363–9.
18. Vallorosi CJ, Day KC, Zhao X, Rashid MG, Rubin MA, Johnson KR, *et al.* Truncation of the β-catenin binding domain of

E-cadherin precedes epithelial apoptosis during prostate and mammary involution. J Biol Chem 2000;5:3328–34.
19. Miller JR, Moon RT. Signal transduction through beta-catenin and specification of cell fate during embryogenesis. Genes Dev 1996;10:2527–39.
20. Peifer M. Beta-catenin as oncogene: The smoking gun. Science 1997;275:1752–3.
21. Day ML, Zhao X, Vallorosi CJ, Putzi M, Powell CT, Lin C, *et al.* E-cadherin mediates aggregation-dependent survival of prostate and mammary epithelial cells through the retinoblastoma cell cycle control pathway. J Biol Chem 1999;274:9656–64.
22. Whitehead I, Kirk H, Kay R. Expression cloning of oncogenes by retroviral transfer of cDNA libraries. Mol Cell Biol 1995; 15:704–10.
23. Graff JR, Gabrielson E, Fujii H, Baylin SB, Herman JG. Methylation patterns of the E-cadherin 5' CpG island are unstable and reflect the dynamic, heterogeneous loss of E-cadherin expression during metastatic progression. J Biol Chem 2000; 4:2727–32.
24. Moll R, Mitze M, Frizen U, Birchmeier W. Differential loss of E-cadherin expression in infiltrating ductal and lobular breast carcinomas. Am J Pathol 1993;143:1731–42.
25. Rimm D, Sinard J, Morrow J. Reduced alpha-cadherin and E-cadherin expression in breast cancer. Lab Invest 1995;5: 506–12.
26. Berx G, Cleton-Jansen A-M, Nollet F, de Leeuw WJ, van de Vijver M, Cornelisse C, *et al.* E-cadherin is a tumour/invasion suppressor gene mutated in human lobular breast cancers. EMBO J 1995;14:6107–115.
27. Berx G, Cleton-Jansen A-M, Strumane K, Berx G, Cleton-Jansen AM, Strumane K, *et al.* E-cadherin is inactivated in a majority of invasive human lobular breast cancers by truncation mutations throughout its extracellular domain. Oncogene 1996;13:1919–25.

Mitogen activated protein kinase pathway is involved in RhoC GTPase induced motility, invasion and angiogenesis in inflammatory breast cancer.

Kenneth L. van Golen, Li Wei Bao, Quintin Pan, Fred R. Miller[1], Zhi Fen Wu, Sofia D. Merajver[2]

Department of Internal Medicine, University of Michigan Comprehensive Cancer Center and [1]Breast Cancer Program, Barbara Ann Karmanos Cancer Institute

Running Title: Downstream RhoC GTPase Signaling in Inflammatory Breast Cancer.

Key Words: angiogenic factors, C3 exotransferase, human mammary epithelial (HME) cells, inflammatory breast cancer (IBC), inhibitors, invasion, mitogen activated protein kinase (MAPK), motility, phosphatidylinositol-3 kinase (PI3K), RhoC GTPase,

Abbreviations: inflammatory breast cancer (IBC), human mammary epithelial (HME), mitogen activated protein kinase (MAPK), phosphatidylinositol-3 kinase (PI3K), locally advanced breast cancer (LABC), fetal bovine serum (FBS), vascular endothelial growth factor (VEGF), 3-[4,5-Dimethylthiazol-2-yl]-2,5-diphenyltetrazolium bromide (MTT), enzyme linked immunoabsorbant assay (ELISA), minimal essential medium (MEM), tricholoracetic acid (TCA), interleukin (IL), basic fibroblast growth factor (FGF2) fibroblast growth factor binding protein (FGF-BP), insulin-like growth factor binding protein related protein (IGFBP-rP).

[2]*Correspondence to*: Sofia D. Merajver, M.D., Ph.D. 7217 CCGC 1500 East Medical Center Drive, Ann Arbor, MI 48109-0948 smerajve@umich.edu

Abstract

Inflammatory breast cancer (IBC) is the most lethal form of locally advanced breast cancer known. IBC carries a guarded prognosis primarily due to rapid onset of disease, typically within 6 months, and the propensity of tumor emboli to invade the dermal lymphatics and spread systemically. Although the clinical manifestations of IBC have been well documented, until recently little was known about the genetic mechanisms underlying the disease. In a comprehensive study aimed at identifying the molecular mechanisms responsible for the unique IBC phenotype, our laboratory identified overexpression of RhoC GTPase in over 90% of IBC tumors in contrast to 36% of stage-matched non-IBC tumors. We also demonstrated that overexpression of RhoC GTPase in human mammary epithelial (HME) cells nearly recapitulated the IBC phenotype with regards to invasion, motility and angiogenesis. In the current study we sought to delineate which signaling pathways were responsible for each aspect of the IBC phenotype. Using well-established inhibitors to the mitogen activated protein kinase (MAPK) and phosphatidylinositol-3 kinase (PI3K) pathways. We found that activation of the MAPK pathway was responsible for motility, invasion and production of angiogenic factors. In contrast, growth under anchorage independent conditions was dependent on the PI3K pathway.

Introduction

Inflammatory breast cancer (IBC) is a phenotypically distinct form of locally advanced breast cancer (LABC) that accounts for approximately 6% of new breast cancer cases annually in the United States [1]. Because of the rapid onset of disease, typically within 6 months, and the propensity of IBC to invade, grow and spread in the dermal lymphatics of the skin overlying the breast, IBC carries with it the worst prognosis of all LABCs [2;3]. It is the ability of the tumor emboli to invade and block the dermal lymphatics that leads to the primary skin changes associated with IBC [1-4].

Although the clinical manifestations of IBC have been well documented in the literature, until recently little was known about the molecular mechanisms involved in conferring the unique IBC phenotype. In an effort to identify genetic alterations involved in determining the IBC phenotype, our laboratory isolated two genes that were consistently and concordantly altered in IBC compared with stage-matched non-IBC tumors [5]. Expression of a novel tumor suppressor gene, termed LIBC (for Lost in Inflammatory Breast Cancer; also known as Wisp3 and IGFBP-rP9), was found to be lost in a significant proportion of IBC tumors compared with non-IBC stage-matched LABC specimens. Conversely, RhoC GTPase, was over-expressed in 90% of IBC tumors versus 36% of the stage-matched controls.

RhoC GTPase is a member of the Ras-superfamily of small GTP binding proteins and is primarily responsible for re-organization of the actin cytoskeleton leading to cellular motility [6-12]. In addition, Rho proteins can also give rise to or modulate formation of lamellipodia and fillipodia, cellular proliferation and p53-

independent/bcl2-dependent apoptosis [13]. Transfection of the RhoC homologue, RhoB, into Ras-transformed NIH3T3 cells leads to increased focus formation suggesting a role for the Rho proteins as a transforming oncogene or as a metastasis gene [14]. Similarly, our laboratory has demonstrated that overexpression of RhoC in immortalized HME cells leads to a tumorigenic phenotype that resembles IBC [15-17]. Specifically, RhoC transfected HME cells become highly motile and invasive, grow under anchorage independent conditions, produce angiogenic factors, and are tumorigenic and metastatic when orthotopically implanted into nude mice [15;17].

These *in vitro* data have additional clinical significance. In addition to IBC, RhoC overexpression also correlates with a poor prognosis in pancreatic adenocarcinoma, is required for hepatic metastasis, and is associated with the transition to metastatic disease in melanoma [18-20]. The role of RhoC in human cancer has recently generated increased interest. It has been proposed that Rho proteins act through and potentiate signaling via the mitogen activated protein kinase (MAPK) pathway (reviewed by Takai et. al.) [21]. Evidence from other laboratories suggest that Rho proteins can signal through both the MAPK pathway as well as the phosphoinositol-3 kinase (PI3K) pathway [22-25]. Furthermore, it has been demonstrated that in certain cell types, the MAPK pathway is involved in signaling and the production of angiogenic factors while the PI3K pathway is involved in growth and survival [26-33].

In our present study we set out to determine the major pathways involved in RhoC signaling in IBC. Specifically, we attempted to determine which arms

and/or pathways were involved in conferring specific aspects of the RhoC-induced phenotype. Many of the published studies that describe the signal transduction pathways involved in Rho signaling were performed in transfected NIH3T3 cells, thus our study focused on the RhoC signaling pathways specific to IBC and HME cells. We treated HME-RhoC stable transfectants, HME-β-galactosidase (HME-β-gal) control transfectants or the SUM149 IBC cell line with C3 exotransferase (a specific inhibitor of Rho proteins), a variety of MAPK inhibitors, or a PI3K inhibitor and assayed them for specific biological functions. The inhibitors were used at concentrations that would inhibit signal transduction without affecting cellular growth. We found that the PI3K pathway was involved in anchorage independent growth and survival, while multiple arms of the MAPK pathway were involved in motility and invasion, and that p38 is a downstream modulator in the production of angiogenic factors. These data provide significant new insight as to how overexpression of RhoC can lead to a variety of phenotypic effects in breast cells.

Materials and methods

Cell culture

Cell lines were maintained under defined culture conditions for optimal growth in each case [34-36]. Briefly, human mammary epithelial (HME) cells were immortalized with human papilloma virus E6/E7 [37] and grown in 5% fetal bovine serum (FBS; Sigma Chemical Co., St. Louis, MO) supplemented Ham's

F-12 medium (JRH BioSciences, Lenexa, KS) containing insulin, hydrocortisone, epidermal growth factor, and cholera toxin (Sigma Chemical Co.). Stable HME transfectants containing either the human RhoC GTPase or control β-galactosidase genes were maintained in the described medium supplemented with 100 μg/ml hygromycin (LifeScience Technologies). The SUM149 cell line was developed from a primary IBC tumor and grown in 5% FBS supplemented Ham's F-12 medium containing insulin and hydrocortizone. The HME cells were characterized as being keratin 19 positive, ensuring that they are from the same differentiation lineage as the SUM149 IBC tumor cell line.

Cells actively growing in culture were treated with MAPK inhibitors, 2.0 μM PD98059, 1.5 μM U0126, 1.5 μM SKF86002, or 1.5 μM SB220025 (all obtained from Calbiochem, San Diego, CA) 24 h prior to assays and treated everyday with fresh inhibitor until the end of the assay. Treatment of cells with 2.5 μM LY294002 (Calbiochem), a PI3K inhibitor, was performed in the same manner as described for the MAPK inhibitors. These concentrations were below the IC_{50} of the compounds to avoid direct cell toxicity to allow for meaningful biological assays.

Western blot analysis

Proteins were harvested from cell cultures using RIPA buffer (1x PBS, 1% Nonidet P-40, 0.5% sodium deoxycholate, 0.1% SDS, 0.1 mg/ml PMSF, 1 mM sodium orthovanadate and 0.3 mg/ml aprotinin; Sigma Chemical Co.) Ten μg

aliquots were mixed with Laemelli buffer, heat denatured for 3 min, separated by SDS-PAGE, and transferred to nitrocellulose. Non-specific binding was blocked by overnight incubation with 2% powdered milk in tris-buffered saline with 0.05% Tween-20 (Sigma Chemical Co.). Immobilized proteins were probed using antibodies specific for total MAPK proteins and phosphorylated MAPK proteins. Specifically, p38/pp38, pJNK/ppJNK, and pErk/ppErk (Cell Signaling Technologies, Beverly, MA). Protein bands were visualized by ECL (Amersham-Pharmacia Biotech, Piscataway, NJ).

C3 exotransferase treatment

Active C3 exoenzyme was introduced into the HME, HME-β-gal, HME-RhoC, and SUM149 cells using a method based on liposome encapsulation and membrane fusion, which we have termed lipoporation. Briefly, cells were grown in 6-well plates until reaching a confluence of 40–50% and the medium replaced with fresh medium. Three micrograms of human recombinant C3 exotransferase (Cytoskeleton Inc., Denver, CO) was combine with FuGene™ 6 transfection reagent (Roche-Boehringer Mannheim) and added to the cultures. As controls either an equal quantity of human recombinant tubulin or FuGene™ 6 alone were added to cell cultures. The cells were incubated for 2 days at 37°C, at which time cell-conditioned medium was harvested. Presence of the intracellular C3 exoenzyme was confirmed by visualizing the rhodamine-tagged protein using fluorescent microscopy. The efficiency and activity of both the transfected and

lipoporated C3 exoenzyme were confirmed by a quantitative ADP-ribosylation assay [38].

The efficiency of in vivo ADP-ribosylation of RhoC GTPase by C3 exotransferase was determined as previously described [16]. Active C3 exotransferase was efficiently introduced into HME-β-gal, HME-RhoC, and SUM149, as described above. Cells were collected 48 hours later, washed in medium, and pelleted. The cells were lysed in 20 mM HEPES pH 8.0 (Sigma Chemical Co.) by 3 repeated freeze/thaw cycles. Cell lysates (10 μg) were combined with 50 ng/ml C3 exotransferase and 5 x 10^6 cpm [^{32}P]NAD (Amersham) in ADP-ribosylation buffer (20 mM HEPES, pH 8.0, 1 mM $MgCl_2$, 1 mM AMP and thymadine, Sigma Chemical Co.), and incubated for 30 min at 37°C. TCA-perceptible material was then recovered and radioactivity was counted on a Packard scintillation counter.

Growth assays

Monolayer culture growth rate was determined as previously described [39] by conversion of MTT (3-[4,5-Dimethylthiazol-2-yl]-2,5-diphenyltetrazolium bromide; Sigma Chemical Co.) to a water insoluble formazon by viable cells. Three thousand cells in 200 μl medium were plated in 96-well plates and grown under normal conditions. Cultures were assayed at 0, 1, 2, 3, 5 and 7 days by the addition of 40 μl 5mg/ml MTT and incubating for 1h at 37°C. The MTT containing medium was aspirated and 100 μl DMSO (Sigma Chemical Co.) added to lyse

the cells and solublize the formazon. Absorbance values of the lysates were determined on a Dynatech MR 5000 microplate reader at 540 nm.

For anchorage independent growth assays, a 2% stock of sterile low-melt agarose was diluted 1:1 with 2x MEM. Further dilution to 0.6% agarose was made using 10% FBS supplemented Ham's F-12 medium complete with growth factors, and 1 ml was added to each well of a six-well plate as a base-layer. The cell layer was then prepared by diluting agarose to 0.3% and 0.6% with 10^3 cells in 2.5% FBS supplemented Ham's F-12/1.5 ml/well. Colonies greater than or equal to 100 μ in diameter were counted after a 3-week incubation at 37°C in a 10% CO_2 incubator.

Random motility assay

Random motility was determined using a gold-colloid assay [40]. Gold-colloid (Sigma Chemical Co.) was layered onto glass coverslips and placed into 6-well plates. Cells were plated onto the coverslips and allowed to adhere for 1 h at 37°C in a CO_2 incubator (12,500 cells/3 ml in serum-free medium). To stimulate the cells, the serum-free medium was replaced with 5% FBS containing Ham's F-12 supplemented with growth factors and allowed to incubate for 3 h at 37°C. The medium was aspirated and the cells fixed using 2% gluteraldehyde (Sigma Chemical Co.). The coverslips were then mounted onto glass microscope slides and areas of clearing in the gold-colloid corresponding to phagokinetic cell tracks counted.

Invasion assay

The invasion assay was performed as previously described with minor modification [39]. A 10 µl aliquot of10 mg/ml Matrigel (Becton Dickenson, Bedford, MA) was spread onto a 6.5 mm Transwell filter with 8 µm pores (Costar, Corning, NY) and air dried in a laminar flow hood. Once dried, the filters were reconstituted with a few drops of serum-free medium. The lower chamber of the Transwell was filled with either serum-free or serum containing media. Cells were harvested and resuspended in serum-free medium with 0.1% BSA at a concentration of 3.75×10^5 cells/ml and 0.5 ml was added to the top chamber. The chambers were incubated for 24 h at 37°C in a 10% CO_2 incubator. The cell suspension was aspirated and excess Matrigel removed from the filter using a cotton swab. The filters were then cut away from the Transwell assembly and fixed with methanol, gel side down, to a glass microscope slide. The fixed filters were stained with hematoxylin and eosin, and the cells in 20 random 40x-magnification fields counted. These cells were assumed to have invaded through the Matrigel and filter. The number of cells that had invaded in the serum-free containing lower chambers was considered background and this number was subtracted from the number of cells that had invaded in response to the serum-containing medium.

Quantitation of vascular endothelial growth factor

Levels of soluble cytokines and chemokines were determined from cell-conditioned media. Cells were incubated in normal growth medium for 4 days. The cell-conditioned media was harvested, centrifuged for 5 min at 2,500 rpm and divided into 1 ml aliquots. The Quantikine human vascular endothelial growth factor (hVEGF; R&D Systems, Minneapolis, MN) were used to measure protein levels of the 165 amino acid species of hVEGF. The enzyme linked immunoabsorbant assay (ELISA) was performed per the manufacturers recommendations.

Results

C3 exotransferase inhibition of RhoC GTPase

In a previous study we demonstrated that inhibition of RhoC GTPase activity by C3 exotransferase treatment led to decreased production of angiogenic factors [16;17]. In order to demonstrate that the other phenotypic changes seen in the HME-RhoC transfectants are indeed due to RhoC expression, we treated the cells with C3 exotransferase. C3 exotransferase is not a specific inhibitor of RhoC *per se*, but a general inhibitor of Rho proteins (reviewed in [41]). However, given that the untransfected HME, the HME-β-galactosidase control transfectants, and the HME-RhoC transfected cells were all derived from the same culture, they are likely to share the same distribution of Rho proteins,

except for RhoC. Therefore, main changes of phenotype produced by C3 treatment would be ascribed to changes in RhoC GTPase activity.

Active C3 exotransferase was introduced into the cells using a liposome mediated method termed lipoporation [16]. As shown in Table 1, the population doubling time of all the cell lines tested was not significantly affected by C3 treatment. However, the ability of the HME-RhoC transfectants and the SUM149 IBC cell line to grow under anchorage independent conditions, a hallmark of malignant transformation, was significantly reduced. In contrast, C3 treatment of the HME untransfected or the HME-β-gal control did not result in any changes in their ability to grow in soft agar. The monolayer growth rate was not influenced by transfection or RhoC expression, the HME-RhoC transfectants did not differ from the untransfected or control transfected HME counterparts, or by C3 treatment so, these data suggest that RhoC confers the ability to HME-RhoC cells to grow under anchorage independent conditions.

As demonstrated in Figure 1A, C3 treatment significantly reduced HME-RhoC and SUM149 IBC motility in a random colloidal gold assay. The HME-β-galactosidase control transfectants were unaffected by C3 treatment. Similarly, the ability of the HME-RhoC and SUM149 cells to invade a Matrigel coated filter in response to a chemoattractant was significantly reduced after C3 treatment (Figure 1B).

The activity of the C3 exotransferase was confirmed by measuring the efficiency of *in vivo* ADP-ribosylation. As shown in Figure 1C, in comparison with their non-C3 treated counterparts, all the C3 treated cell lines had a significant

reduction in the levels of available sites that could be ADP-ribosylated in the *in vitro* assay. Specifically, the C3-treated HME-RhoC and SUM149 cells had a 2-fold decrease in the number of ADP-ribosylated sites compared to the non-transfected controls. These data indicate that at least half of the Rho proteins have been ADP-ribosylated *in vivo*, and therefore inhibited by C3 exotransferase. Taken together, these data demonstrate that expression and activity of RhoC GTPase is responsible for conferring the ability to grow under anchorage independent conditions, and the production of a motile and invasive cell.

Inhibition of anchorage independent growth by the LY294002 PI3K inhibitor

To determine whether the PI3K or the MAPK pathways were involved in RhoC signaling, we treated the cells with either LY294002 (a potent PI3K inhibitor) or PD98059 (a general MAPK inhibitor that blocks all arms of the MAPK pathway). To avoid confounding effects due to direct cytotoxicity, we chose concentrations of the inhibitors that inhibited signal transduction but were not cytotoxic. The cells were treated 48 h prior to plating in 0.6% soft agar and fresh medium containing each of the inhibitors was layered onto the soft agar daily. The MCF10AT c1 cell line, with a constituitvely active Ras was used as a positive control [42]. The ability of the HME-RhoC and SUM149 cells to form colonies in 0.6% soft agar was significantly reduced by treatment with the PI3K inhibitor (Figure 2). In contrast, treatment with the general MAPK inhibitor PD98059 had little effect on the colony number. The reduction in colony formation was not due

to a significant change in the population doubling time of the cells treated with LY294002, as determined by an MTT monolayer growth assay (data not shown). These data indicate the PI3K pathway, and not the MAPK pathway is involved in RhoC conferring the ability of the cells to survive and form colonies under anchorage independent conditions.

MAPK status in cell lines after inhibitor treatment

In order to determine which arms of the MAPK pathway were involved in the different aspects of the RhoC-induced phenotype, the cells were treated with a variety of MAPK inhibitors that affect different points of the pathway. The general MAPK inhibitor PD98059 effects the MAPK pathway at 3 distinct, points; 1) MEK3 (which activates p38), 2) MEKK-1 (which activates p38 and MEK1 &2, and therefore ERK1 & 2), 3) MEK4 (which activates JNK). The inhibitor U0126 inhibits MEK1 & 2, and therefore also, ERK1 & 2 activation. The inhibitors SKF86002 and SB22025 are inhibitors of p38 activation and of p38 itself, respectively. As demonstrated in Figure 3, all cell lines expressed p38, ERK (p42/p44), and JNK. However, none of the untreated cell lines (A) expressed activated phospho-JNK, suggesting that only pp38 and phospho-ERK are involved in RhoC signal transduction. Treatment of the cells for 24 h with SKF86002 (B), PD98059 (C), U0126 (D), or C3 exotransferase (E), led to a decrease in the levels of the active phosphorylated form of the target protein(s),

while the basal levels remained unchanged. Interestingly, C3 treatment of the cells lead to increased phosphorylation of JNK.

Effect of inhibition of MAPK on motility and invasion

Because of the postulated relationship between Rho induced motility and Ras activation of the MAPK pathway, we set out to understand how are the MAPK signaling branches involved in Rho-modulated motility and invasion. To accomplish this we treated the cells with the various MAPK inhibitors described above. The cells were treated with the MAPK inhibitors 48 h prior to assessing motility and invasion. No significant decrease in population doubling time was observed for the cells treated with inhibitors (data not shown).

As demonstrated in Figure 4A, all of the MAPK inhibitors had a significant ($p=0.01$) effect on the motility of the HME-RhoC and SUM149 cell lines. The areas of the phagokinetic tracks were reduced to nearly the level of the HME-β-gal control cell line, which was unaffected by any of the MAPK inhibitors. Since all of the MAPK inhibitors had an effect on the motility of the cells, this suggested that multiple arms of the MAPK pathway are involved in RhoC mediated motility. Motility of the MCF10AT c1 positive control cell line that has a constituatively active Ras was also affected by all four of the MAPK inhibitors, although the motility of these cells is much reduced compared to the HME-RhoC and SUM149 cells.

Next, we concentrated on the cells ability to invade through a Matrigel coated filter (Figure 4B). The invasive capabilities of the cells are described as fold-increase in invasion over untransfected HME controls. Treatment with all four of the MAPK inhibitors reduced the invasive capabilities of the HME-RhoC and SUM149 cell lines. The HME-β-gal control cells were not significantly affected, by the other MAPK inhibitors. The invasive capabilities of the MCF10AT c1 cells were the same as the HME-β-gal control cells, and were likewise unaffected by the MAPK inhibitors. When cells were treated with a combination of the LY294002 and PD98059 inhibitors, the level of inhibition is similar to that of the PD98059 inhibitor alone (data not shown), suggesting that the PI3K pathway is not involved in either motility or invasion.

Taken together, these data suggest that RhoC induced motility and invasion is mediated to a significant extent by the p38 and ERK arms of the MAPK pathway. This is shared with Ras alone induced motility, but active Ras is not sufficient to produce an invasive phenotype in the MCF10A cells. In all these experiments the concentrations of inhibitors used did not effect cell doubling times or cell viability.

VEGF production after inhibition of the MAPK pathway

In a previous study, we demonstrated that RhoC overexpression can lead to increased production of angiogenic factors such as vascular endothelial growth factor (VEGF) [16]. Treatment of the mammary cells with the different MAPK

inhibitors resulted in decreased VEGF production by the HME-RhoC and SUM149 IBC cell lines (Figure 5). The greatest reduction in VEGF production was seen when the cells were treated with the inhibitor SB22025, which prevents p38 activation. Treatment with the inhibitor SKF86002, an inhibitor of phosho-p38 activity, resulted in the second greatest decrease in VEGF production. Taken together, these data suggest that activation of the p38 arm of the MAPK pathway is responsible for production of VEGF simultaneously by RhoC overexpression.

Discussion

The highly invasive and metastatic phenotype of IBC is one of the hallmarks of its unique clinical manifestations and the major cause of the poor outcome of many patients who are diagnosed with IBC. In a previous set of studies, our laboratory identified RhoC GTPase to be over-expressed in IBC [5]. Furthermore, we demonstrated RhoC GTPase overexpression results in an IBC-like phenotype [15-17]. Specifically, the cells are able to grow under anchorage independent conditions, become motile and invasive, produce angiogenic factors, and are able to form tumors and metastases in athymic nude mice.

In the current study, we sought to begin to delineate the signaling pathways responsible for each phenotypic aspect produced by RhoC expression. We hypothesized that in order for RhoC GTPase to achieve diverse phenotypic attributes, cell signaling must take place through several signal transduction

pathways. We utilized specific inhibitors of different points of the PI3K and MAPK pathways, an approach which has proven successful in similar previous studies [43;44].

The MAPK pathway has been previously implicated in Ras and Rho signaling, and it has been suggested that Rho family members (RhoA, Rac1, and cdc42) signal through both the MAPK, and the PI3K pathways (reviewed in [45;46]). Both pathways, depending on cell type, have been attributed to participate in growth/survival and motility (reviewed in [29]). However, many of the published data on RhoA, Rac1, and cdc42 signal transduction pathways, have not been performed in breast cancer cells, specifically those with a Rho-associated phenotype. To date, the signal transduction pathway(s) utilized by RhoC during motility and invasion has not been described in any cell type. In the current study we examined RhoC signal transduction in the SUM149 IBC and HME-RhoC breast cell lines. Because RhoC appears to be a major determinant of a clinically well-defined mammary cancer phenotype it is especially relevant to understand how RhoC elicits multiple actions in breast tissue.

Using MAPK and PI3K inhibitors at concentrations below cytotoxic and cytostatic levels, we have determined that the PI3K pathway is involved in the ability of RhoC overexpressing cells to grow under anchorage independent conditions, while their monolayer population doubling time remained unchanged. We also determined that signaling through the MAPK pathway is involved in motility, invasion and the production of angiogenic factors. Specifically, we found that the ERK and p38 arms of the MAPK signaling complex are involved in

motility and invasion, as no one inhibitor of the individual arms completely blocked motility of the HME-RhoC or SUM149 IBC cell lines. In addition, we know that JNK does not appear to be involved because although it is expressed by the cells, it is not phosphorylated or active in any of the breast lines (IBC or HME) studied. Interestingly, JNK phosphorylation was observed in all cell lines in response to C3 exotransferase treatment, however, phospho-JNK failed to rescue any aspect of the RhoC phenotype that were inhibited by C3 exoenzyme.

The quantitative role played by each part of the MAPK pathway is not yet known. The most potent and best characterized inhibitors, such as PD98059 and U0126, affect molecules upstream and therefore have a broader effect on the MAPK pathway. However, using inhibitors specific for p38, we found that activation of p38 was a modulator for the production of angiogenic factors in these cells. The combination of MAPK inhibitors and the PI3K inhibitor did not result in a further decrease in motility, invasion or production of angiogenic factors, thus suggesting that MAPK signaling is nearly exclusively responsible for producing these phenotypic attributes.

Previous experiments have demonstrated that the various signal transduction pathways have diverse effects in different cell types activated by a variety of stimuli. For example in Schwann cells, PI3K activation by Rac1 leading to lamellipodia formation and motility has been shown to occur upon stimulation by insulin-like growth factor-I [25]. Whereas stimulation of adipocytes with insulin leads activation of the PI3K pathway and Rho-mediated glucose uptake [47]. In support of our data, Amundadottir and Leder demonstrated that regardless of the

oncogene involved in transformation, the PI3K pathway was involved in conferring anchorage independent growth to transformed mammary epithelial cells [48]. They also demonstrated that anchorage independent growth of mammary cells transformed by Her2/neu, v-Ha-ras, and c-myc, could not be inhibited by treatment with the MAPK inhibitor PD98059. Thus consistently in the case of our RhoC expressing cells, it appears that the PI3K pathway is exclusively involved in conferring anchorage independent growth, without involving the MAPK pathway.

Several studies have demonstrated that activation of the MAPK pathway can lead to cell migration and invasion of fibroblasts, keratinocytes and endothelial cells [49-51]. Further, it has been well documented that the Rho proteins can activate the MAPK cascade stimulating various aspects of cellular motility [29;52-54]. Rac1 and cdc42 have been shown to signal gene transcription through JNK and RhoA through p38, or when bound to fibronectin, ERK [22;52;55;56]. Like RhoA, we have made similar observations for RhoC as we have demonstrated activation of both p38 and ERK, but not JNK, in IBC and transfected HME cells. During motility, a dynamic interplay between Rac1, cdc42 and Rho must occur to form lamellipodia, fillipodia, focal adhesions, and stress fibers [7;57;58]. "Cross-talk" between these molecules results in reciprocal activation of Rho with Rac1 and cdc42 [57;59;60]. Therefore, each arm of the MAPK pathway may be involved in motility and invasion.

In a previous study we demonstrated that levels of VEGF was elevated due to RhoC overexpressing cells [16]. Several studies have demonstrated that

activation of angiogenic factors is mediated by the p38 MAPK pathway [26-28]. An increasing body of evidence suggests that the mode of VEGF induction (i.e. MAPK vs. PI3K) by activated H-*ras* is a cell-type specific process, with cells of epithelial origin signaling more commonly through the MAPK pathway whereas those of mesodermal origin utilizing the PI3K pathway [61]. Stimulation of a variety of breast cancer cell lines with heregulin results in activation of p38 and subsequent upregulation of VEGF expression and secretion [28]. Similarly, epidermal growth factor stimulation of squamous cell carcinoma cell lines, results in activation of both p38 and ERK, which in turn, leads to expression of fibroblast growth factor-binding protein (FGF-BP), a potent angiogenic modulator [26]. Furthermore, it has been suggested that Rho proteins and the p38-MAP kinase pathway modulate IL-8 expression [62;63;63]. IL-8 expression has profound biological consequences: it is a potent angiogenic, mitogenic and chemotactic factor in several malignancies including breast and prostate cancer [64-68]. Still others have suggested that bFGF, acting in an autocrine and paracrine fashion, can induce IL-6 expression through p38. In future studies we will determine whether IL-6, IL-8, and FGF2 production is also modulated by the p38 pathway in RhoC overexpressing mammary cells.

In conclusion, we have begun to identify the different signal transduction pathways involved in RhoC GTPase driven phenotypes associated with highly metastatic inflammatory breast cancer. We specifically demonstrated that anchorage independent conditions is mediated via the PI3K pathway. Induction of motility and invasion are mediated through activation of the ERK and p38 arms

of the MAPK pathway, and the production of VEGF is mediated primarily by p38 activation. This study provides new insight into the signal transduction pathways of an aggressive disease mediated by overexpression and activation of RhoC GTPase and suggests new potential targets for therapeutic interventions focused on the biological actions of RhoC.

Acknowledgements

This work was supported by the National Cancer Institute grant R01 CA 77612 (S. D. M.), DAMD 17-00-1-0345, from The Department of Defense, U.S. Army Breast Cancer Program (S. D. M.) and 5T32 CA 09537 (to S. D. M.) and a post-doctoral fellowship (to K. L. v. G.) from the Susan G. Komen Breast Cancer Foundation. We would like to thank Ms. L. Robbins for help in preparation of this manuscript.

References

1. Levine PH, Steinhorn SC, Ries LG, Aron JL. Inflammatory breast cancer: The experience of the surveillance, epidemiology, and end results (SEER) program. J Natl Cancer Inst 1985; 74:291-7.

2. Jaiyesimi I, Buzdar A, Hortobagyi G. Inflammatory breast cancer: a review. J Clin Oncol 1992; 10:1014-24.

3. Beahrs O, Henson D, Hutter R. Manual for Staging of Cancer. In: 1988: 145-50.

4. Kleer CG, van Golen KL, Merajver SD. Molecular biology of breast cancer metastasis. Inflammatory Breast Cancer: Clinical Syndrome and Molecular Determinants. Breast Cancer Res 2000; 2:423-9.

5. van Golen KL, Davies S, Wu ZF, Wang Y, Bucana CD, Root H, Chandrasekharappa S, Strawderman M, Ethier SP, Merajver SD. A novel putative low-affinity insulin-like growth factor-binding protein, LIBC (lost in inflammatory breast cancer), and RhoC GTPase correlate with the inflammatory breast cancer phenotype. Clin Cancer Res 1999; 5:2511-9.

6. Ridley A. Membrane Ruffling and Signal Transduction. Bioessays 1994; 16:321-7.

7. Hall A. Rho GTPases and the Actin Cytoskeleton. Science 1998; 279:509-14.

8. Ridley AJ. The GTP-binding Protein Rho. Int J Biochem Cell Biol 1997; 29:1225-9.

9. Esteve P, Embade N, Perona R, Jimenez B, del Peso L, Leon J, Arends M, Miki T, Lacal JC. Rho-regulated signals induce apoptosis *in vitro* and *in vivo* by a p53-independent, but Bc12 dependent pathway. Oncogene 1998; 17:1855-69.

10. Hall A. Small GTP-binding proteins and the regulation of the cytoskeleton. Annu Rev Cell Biol 1994; 10:31-54.

11. Apenstrom P. Effectors for the Rho GTPases. Curr Opin Cell Biol 1999; 11:95-102.

12. Nobes CD, Hall A. Rho, rac, and cdc42 GTPases regulate the assembly of multimolecular focal complexes associated with actin stress fibers, lamellipodia and filopodia. Cell 1995; 81:53-62.

13. Helvie MA, Wilson TE, Roubidoux MA, Wilkins EG, Chang AE. Mammographic appearance of recurrent breast carcinoma in six patients with TRAM flap breast reconstructions. Radiology 1998; 209:711-5.

14. Jimenez B, Arenda M, Esteve P, Perona R, Sanchez R, Cajal S, Wyllie A, Lacal JC. Induction of apoptosis in NIH3T3 cells after serum deprivation by overexpression of *rho*-p21, a GTPase protein of the *ras* superfamily. Oncogene 1995; 10:811-6.

15. van Golen KL, Wu ZF, Qiao XT, Bao LW, Merajver SD. RhoC GTPase, a novel transforming oncogene for human mammary epithelial cells that partially recapitulates the inflammatory breast cancer phenotype. Cancer Res 2000; 60:5832-8.

16. van Golen KL, Wu ZF, Qiao XT, Bao LW, Merajver SD. RhoC GTPase Overexpression Modulates Induction of Angiogenic Factors in Breast Cells. Neoplasia 2000; 2:418-25.

17. van Golen KL, Wu ZF, Bao LW, Merajver SD. RhoC GTPase induces a motile and invasive phenotype in inflammatory breast cancer. Clinical & Experimental Metastasis 1999; 17, 745 (abstract #2.7).

18. Suwa H, Ohshio G, Imamura T, Watanabe G, Arii S, Imamura M, Narumiya S, Hiai H, Fukumoto M. Overexpression of the *rhoC* gene correlates with progression of ductal adenocarcinoma of the pancreas. Br J Cancer 1998; 77:147-52.

19. Genda T, Sakamoto M, Ichida T, Asakura H, Kojiro M, Narumiya S, Hirohashi S. Cell Motility mediated by rho and Rho-associated protein kinase plays a critical role in intrahepatic metastasis of human hepatocellular carcinoma. Hepatology 1999; 30:1027-36.

20. Clark EA, Golub TR, Lander ES, Hynes RO. Genomic analysis of metastasis reveals an essential role for RhoC. Nature 2000; 406:532-5.

21. Takai Y, Sasaki T, Matozaki T. Small GTP-binding proteins. Physiol Rev 2001; 81:153-208.

22. Danen EH, Sonneveld P, Sonnenberg A, Yamada KM. Dual stimulation of Ras/mitogen-activated protein kinase and RhoA by cell adhesion to fibronectin supports growth factor-stimulated cell cycle progression. J Cell Biol 2000; 151:1413-22.

23. Vojtek AB, Cooper JA. Rho family members: activators of MAP kinase cascades. Cell 1995; 82:527-9.

24. Arozarena I, Aaronson DS, Matallanas D, Sanz V, Ajenjo N, Tenbaum SP, Teramoto H, Ighishi T, Zabala JC, Gutkind JS, Crespo P. The Rho family GTPase Cdc42 regulates the activation of Ras/MAP kinase by the exchange factor Ras-GRF. J Biol Chem 2000; 275:26441-8.

25. Cheng HL, Steinway ML, Russell JW, Feldman EL. GTPases and phosphatidylinositol 3-kinase are critical for insulin-like growth factor-I-mediated Schwann cell motility. J Biol Chem 2000; 275:27197-204.

26. Harris VK, Coticchia CM, Kagan BL, Ahmad S, Wellstein A, Riegel AT. Induction of the angiogenic modulator fibroblast growth factor-binding protein by epidermal growth factor is mediated through both MEK/ERK and p38 signal transduction pathways. J Biol Chem 2000; 275:10802-11.

27. Sodhi A, Montaner S, Patel V, Zohar M, Bais C, Mesri EA, Gutkind JS. The Kaposi's sarcoma-associated herpes virus G protein-coupled receptor up-regulates vascular endothelial growth factor expression and secretion through mitogen-activated protein kinase and p38 pathways acting on hypoxia-inducible factor 1α. Cancer Res 2000; 60:4873-80.

28. Xiong S, Grijalva R, Zhang L, Nguyen NT, Pisters PW, Pollock RE, Yu D. Up-regulation of vascular endothelial growth factor in breast cancer cells by the heregulin-beta1-activated p38 signaling pathway enhances endothelial cell migration. Cancer Res 2001; 61:1727-32.

29. Parise LV, Lee J, Juliano RL. New aspects of integrin signaling in cancer. Semin Cancer Biol 2000; 10:407-14.

30. Downward J. Mechanisms and consequences of activation of protein kinase B/Akt. Curr Opin Cell Biol 1998; 10:262-7.

31. Khwaja A, Rodriguez-Viciana P, Wennstrom S, Warne PH, Downward J. Matrix adhesion and Ras transformation both activate a phosphoinositide 3-OH kinase and protein kinase B/Akt cellular survival pathway. EMBO J 1997; 16:2783-93.

32. Ilic D, Almeida EA, Schlaepfer DD, Dazin P, Aizawa S, Damsky CH. Extracellular matrix survival signals transduced by focal adhesion kinase suppress p53-mediated apoptosis. J Cell Biol 1998; 143:547-60.

33. Tamura M, Gu J, Danen EH, Takino T, Miyamoto S, Yamada KM. PTEN interactions with focal adhesion kinase and suppression of the extracellular matrix-dependent phosphatidylinositol 3-kinase/Akt cell survival pathway. J Biol Chem 1999; 274:20693-703.

34. Ethier SP, Kokeny KE, Ridings JW, Dilts CA. erbB family receptor expression and growth regulation in a newly isolated human breast cancer cell line. Cancer Res 1996; 56:899-907.

35. Ethier SP. Human breast cancer cell lines as models of growth regulation and disease progression. J Mammary Gland Biol Neoplasia 1996; 1:111-21.

36. Sartor CI, Dziubinski ML, Yu CL, Jove R, Ethier SP. Role of epidermal growth factor receptor and STAT-3 activation in autonomous proliferation of SUM-102PT human breast cancer cells. Cancer Res 1997; 57:978-87.

37. Band V, Zajchowski D, Kulesa V, Sager R. Human papilloma virus DNAs immortalize normal human mammary epithelial cells and reduce their growth factor requirements. Proc Natl Acad Sci USA 1990; 87:463-7.

38. Stasia MJ, Vignais PV. In: Abelson JM, Simon MI, eds. Methods in Enzymology. New York: Academic Press, 1995: 324-7.

39. van Golen KL, Risin S, Staroselsky A, Berger D, Tainsky MA, Pathak S, Price JE. Predominance of the metastatic phenotype in hybrids formed by fusion of mouse and human melanoma clones. Clin Exp Metastasis 1996; 14:95-106.

40. Albrecht-Buehler G. The phagokinetic tracks of 3T3 cells. Cell 1977; 11:395-404.

41. Aktories K. Rho proteins: targets for bacterial toxins. Trends Microbiol 1997; 5:282-8.

42. Santner SJ, Dawson PJ, Tait L, Soule HD, Eliason J, Mohamed AN, Wolman SR, Heppner GH, Miller FR. Malignant MCF10CA1 cell lines derived from premalignant human breast epithelial MCF10AT cells. Breast Cancer Res Treat 2001; 65:101-10.

43. Dunn SE, Torres JV, Oh JS, Cykert DM, Barrett JC. Up-regulation of urokinase-type plasminogen activator by insulin-like growth factor-I depends upon phosphatidylinositol-3 kinase and mitogen-activated protein kinase kinase. Cancer Res 2001; 61:1367-74.

44. Cuenda A, Alessi DR. Use of kinase inhibitors to dissect signaling pathways. Methods Mol Biol 2000; 99:161-75.

45. Wymann MP, Pirola L. Structure and function of phosphoinositide 3-kinases. Biochim Biophys Acta 1998; 1436:127-50.

46. Lopez-Ilasaca M. Signaling from G-protein-coupled receptors to mitogen-activated protein (MAP)-kinase cascades. Biochem Pharmacol 1998; 56:269-77.

47. Karnam P, Standaert ML, Galloway L, Farese RV. Activation and translocation of Rho (and ADP ribosylation factor) by insulin in rat adipocytes. Apparent involvement of phosphatidylinositol 3-kinase. J Biol Chem 1997; 272:6136-40.

48. Amundadottir LT, Leder P. Signal transduction pathways activated and required for mammary carcinogenesis in response to specific oncogenes. Oncogene 1998; 16:737-46.

49. Yujiri T, Ware M, Widmann C, Oyer R, Russell D, Chan E, Zaitsu Y, Clarke P, Tyler K, Oka Y, Fanger GR, Henson P, Johnson GL. MEK kinase 1 gene disruption alters cell migration and c-Jun NH2- terminal kinase regulation

but does not cause a measurable defect in NF- kappa B activation. Proc Natl Acad Sci USA 2000; 97:7272-7.

50. Zeigler ME, Chi Y, Schmidt T, Varani J. Role of ERK and JNK pathways in regulating cell motility and matrix metalloproteinase 9 production in growth factor-stimulated human epidermal keratinocytes. J Cell Physiol 1999; 180:271-84.

51. Matsumoto T, Yokote K, Tamura K, Takemoto M, Ueno H, Saito Y, Mori S. Platelet-derived growth factor activates p38 mitogen-activated protein kinase through a Ras-dependent pathway that is important for actin reorganization and cell migration. J Biol Chem 1999; 274:13954-60.

52. Minden A, Lin A, Claret FX, Abo A, Karin M. Selective activation of the JNK signaling cascade and c-Jun transcriptional activity by the small GTPases Rac and Cdc42Hs. Cell 1995; 81:1147-57.

53. Santibanez JF, Iglesias M, Frontelo P, Martinez J, Quintanilla M. Involvement of the Ras/MAPK signaling pathway in the modulation of urokinase production and cellular invasiveness by transforming growth factor-beta(1) in transformed keratinocytes. Biochem Biophys Res Commun 2000; 273:521-7.

54. Royal I, Lamarche-Vane N, Lamorte L, Kaibuchi K, Park M. Activation of cdc42, rac, PAK, and rho-kinase in response to hepatocyte growth factor

differentially regulates epithelial cell colony spreading and dissociation. Mol Biol Cell 2000; 11:1709-25.

55. Coso O, Chiariello M, Yu JC, Teramoto H, Crespo P, Xu N, Miki T, Gutkind JS. The small GTP-binding proteins proteins Rac1 and Cdc42 regulate the activity of the JNK/SAPK signaling pathway. Cell 1995; 81:1137-46.

56. Marinissen MJ, Chiariello M, Gutkind JS. Regulation of gene expression by the small GTPase Rho through the ERK6 (p38 gamma) MAP kinase pathway. Genes Dev 2001; 15:535-53.

57. Small JV, Kaverina I, Krylyshkina O, Rottner K. Cytoskeleton cross-talk during cell motility. FEBS Lett 1999; 452:96-9.

58. Bishop AL, Hall A. Rho GTPases and their effector proteins. Biochem J 2000; 348 Pt 2:241-55.

59. Ridley AJ, Paterson H, Johnston C, Diekman D., Hall A. The small GTP-binding protein rac regulates growth-factor induced membrance ruffling. Cell 1992; 70:401-10.

60. Zondag GCM, Evers EE, ten Klooster JP, Janssen L, van der Kammen RA, Collard JG. Oncogenic Ras downregulates Rac activity, which leads to increased Rho activity and epithelial-mesenchymal transition. J Cell Biol 2000; 149:775-82.

61. Rak J, Mitsuhashi Y, Sheehan C, Tamir A, Viloria-Petit A, Filmus J, Mansour SJ, Ahn NG, Kerbel RS. Oncogenes and tumor angiogenesis: differential modes of vascular endothelial growth factor up-regulation in *ras*-transformed epithelial cells and fibroblasts. Cancer Res 2000; 60:490-8.

62. Warny M, Keates AC, Keates S, Castagliuolo I, Zacks JK, Aboudola S, Qamar A, Pothoulakis C, LaMont JT, Kelly CP. p38 MAP kinase activation by Clostridium difficile toxin A mediates monocyte necrosis, IL-8 production, and enteritis. J Clin Invest 2000; 105:1147-56.

63. Hippenstiel S, Soeth S, Kellas B, Fuhrmann O, Seybold J, Krull M, Eichel-Streiber CV, Goebeler M, Ludwig S, Suttorp N. Rho proteins and the p38-MAPK pathway are important mediators for LPS- induced interleukin-8 expression in human endothelial cells. Blood 2000; 95:3044-51.

64. Rodeck U, Becker D, Herlyn M. Basic fibroblast growth factor in human melanoma. Cancer Cells 1991; 3:308-11.

65. Speirs V, Atkin SL. Production of VEGF and expression of the VEGF receptors Flt-1 and KDR in primary cultures of epithelial and stromal cells derived from breast tumours. Br J Cancer 1999; 80:898-903.

66. Inoue K, Slaton JW, Eve BY, Kim SJ, Perrotte P, Balbay MD, Yano S, Bar-Eli M, Radinsky R, Pettaway CA, Dinney CP. Interleukin 8 expression regulates tumorigenicity and metastases in androgen-independent prostate cancer. Clin Cancer Res 2000; 6:2104-19.

67. Miller LJ, Kurtzman SH, Wang Y, Anderson KH, Lindquist RR, Kreutzer DL. Expression of interleukin-8 receptors on tumor cells and vascular endothelial cells in human breast cancer tissue. Anticancer Res 1998; 18:77-81.

68. Mizuno K, Sone S, Orino E, Mukaida N, Matsushima K, Ogura T. Spontaneous production of interleukin-8 by human lung cancer cells and its augmentation by tumor necrosis factor alpha and interleukin-1 at protein and mRNA levels. Oncology 1994; 51:467-71.

Figure 1. Comparison of the average area of migration in a colloidal gold motility assay by control HME-β-gal and RhoC overexpressing mammary cells after treatment with C3 exotransferase. Treatment of cells with C3 exoenzyme significantly reduced the motile ability of the RhoC overexpressing cells HME-RhoC and SUM149. Similarly, as demonstrated in panel B, the invasive capabilities of the RhoC overexpressing cells were also significantly reduced after C3 treatment as determined in a Matrigel invasion assay. To determine the extent of Rho inhibition by C3 exotransferase, an *in vitro* ADP-ribosylation assay was performed (panel C). The number of ADP-ribosylated targets was greatly reduced in the HME-RhoC and SUM149 cells, thus indicating that C3 exotransferase treatment had effectively blocked the Rho targets within those cells.

Figure 2. Anchorage independent growth in 0.6% soft agar after treatment with either the PI3K inhibitor LY294002 or the general MAPK inhibitor PD98059. The ability of the RhoC overexpressing cells HME-RhoC and SUM149 was significantly reduced after treatment with the LY294002, but not with PD98059. These data suggests that RhoC-mediated anchorage independent growth, is signaled through the PI3K and not the MAPK pathway in these mammary cells.

Figure 3. Western blot analysis of basal and phosphorylated (activated) levels of different arms of the MAPK pathway before (A) and after inhibitor treatment with SKF86002 (B), PD98059 (C), U0126 (D), or C3 exotransferase

(E). All the cell lines tested expressed p38, ERK (p42/p44), and JNK. However, none of the untreated cell lines (A) expressed activated phospho-JNK, suggesting that only pp38 and phospho-ERK are involved in RhoC signal transduction.

Figure 4. Effects on motility and invasion of RhoC overexpressing cells after treatment with PD98059, U0126 or the p38 inhibitor SB220225. Panel A demonstrates a significant decrease in the motility of the RhoC overexpressing HME-RhoC and SUM149 cells treated with the various MAPK inhibitors. Similarly, the ability of these cells to invade through a Matrigel coated filter was also significantly reduced after treatment with the MAPK inhibitors (panel B). These data suggest that RhoC mediated motility and invasion is mediated through the MAPK pathway, to a large extent through activated p38.

Figure 5. The effect of MAPK inhibitors on the production and secretion of the pro-angiogenic molecule vascular endothelial growth factor (VEGF). Production of VEGF by the HME-RhoC and SUM149 cell lines were significantly reduced when the cells were treated with the p38 inhibitors SB220225 or SKF86002. Taken together, these data suggest that activation of the p38 arm of the MAPK pathway is responsible for production of VEGF simultaneously by RhoC overexpression.

Table I.

	Population Doubling Time (hours)		Anchorage Independent Growth (number of colonies)	
	Untreated	C3 Treated	Untreated	C3 Treated
HME	34h	36h	0 ± 0	0 ± 0.1
HME-β-gal	35h	34h	5 ± 0.8	17 ± 7.5
HME-RhoC	33h	36h	102 ± 5.4	40 ± 13.6**
SUM149	39h	39h	75 ± 4.9	47 ± 3.3*

Comparison of monolayer population doubling time and anchorage independent growth of untreated and C3 treated HME, HME transfectants and SUM149 IBC cell lines. Despite treatment of the cells with C3, monolayer population doubling time was not affected. In contrast, the ability of the RhoC expressing HME and SUM149 cells to grow under anchorage independent conditions was significantly reduced (* p=0.01, ** p=0.001).

A

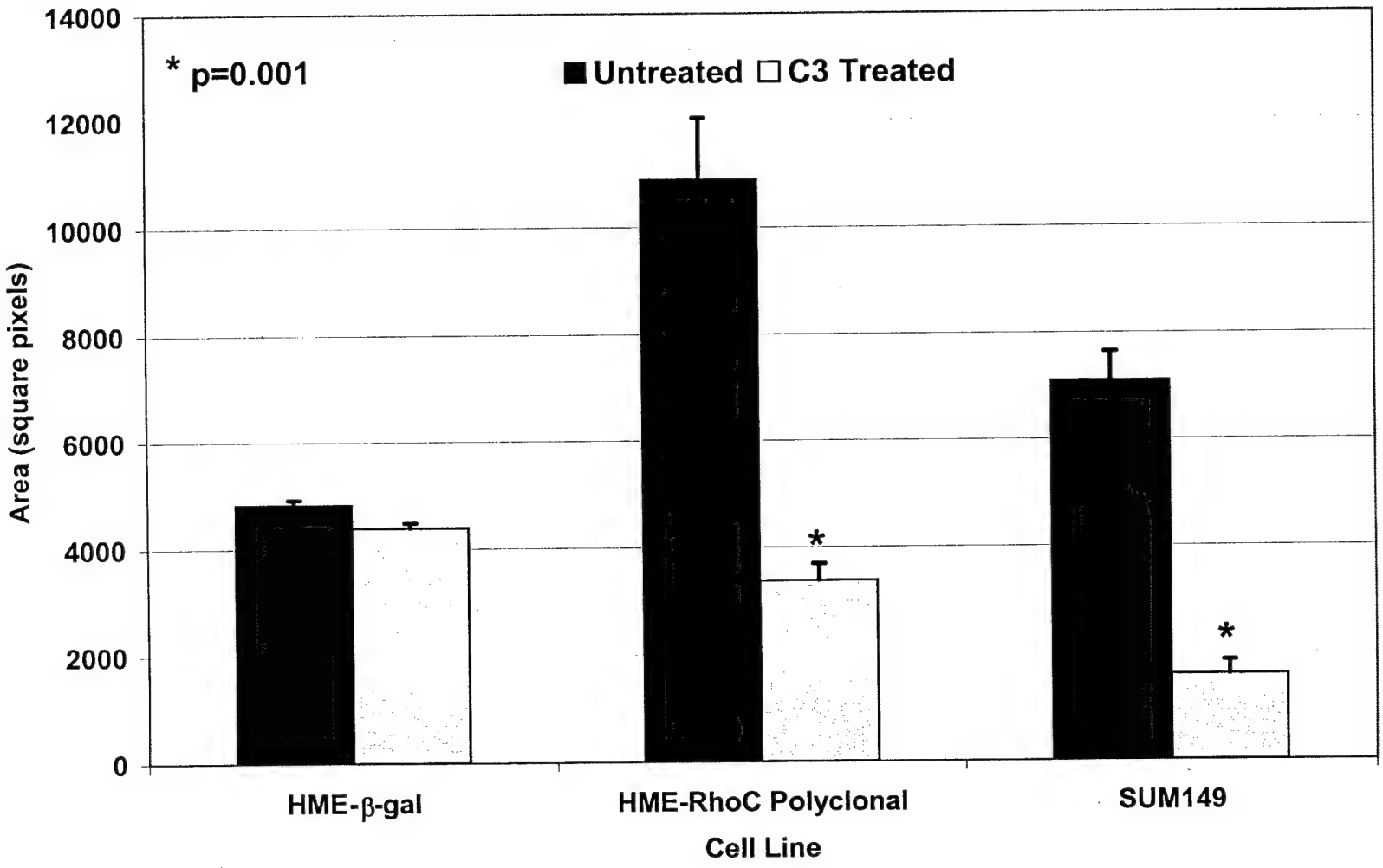
14000
12000
10000
8000
6000
4000
2000
0
* p=0.001
Untreated
C3 Treated
Area (square pixels)
*
*
HME-β-gal
HME-RhoC Polyclonal
SUM149
Cell Line

B

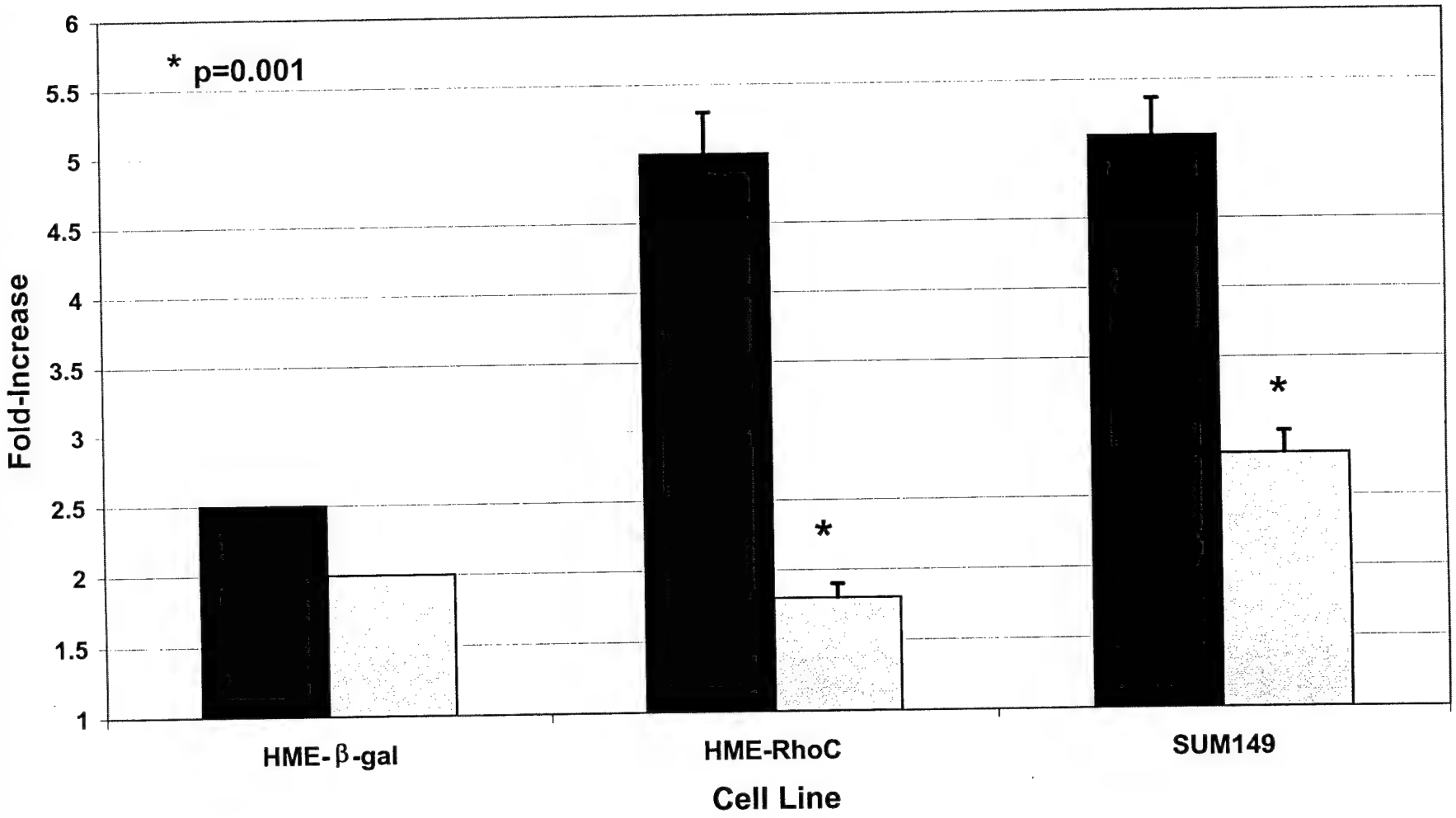
* p=0.001
Fold-Increase
6
5.5
5
4.5
4
3.5
3
2.5
2
1.5
1
*
*
HME-β-gal
HME-RhoC
SUM149
Cell Line

C

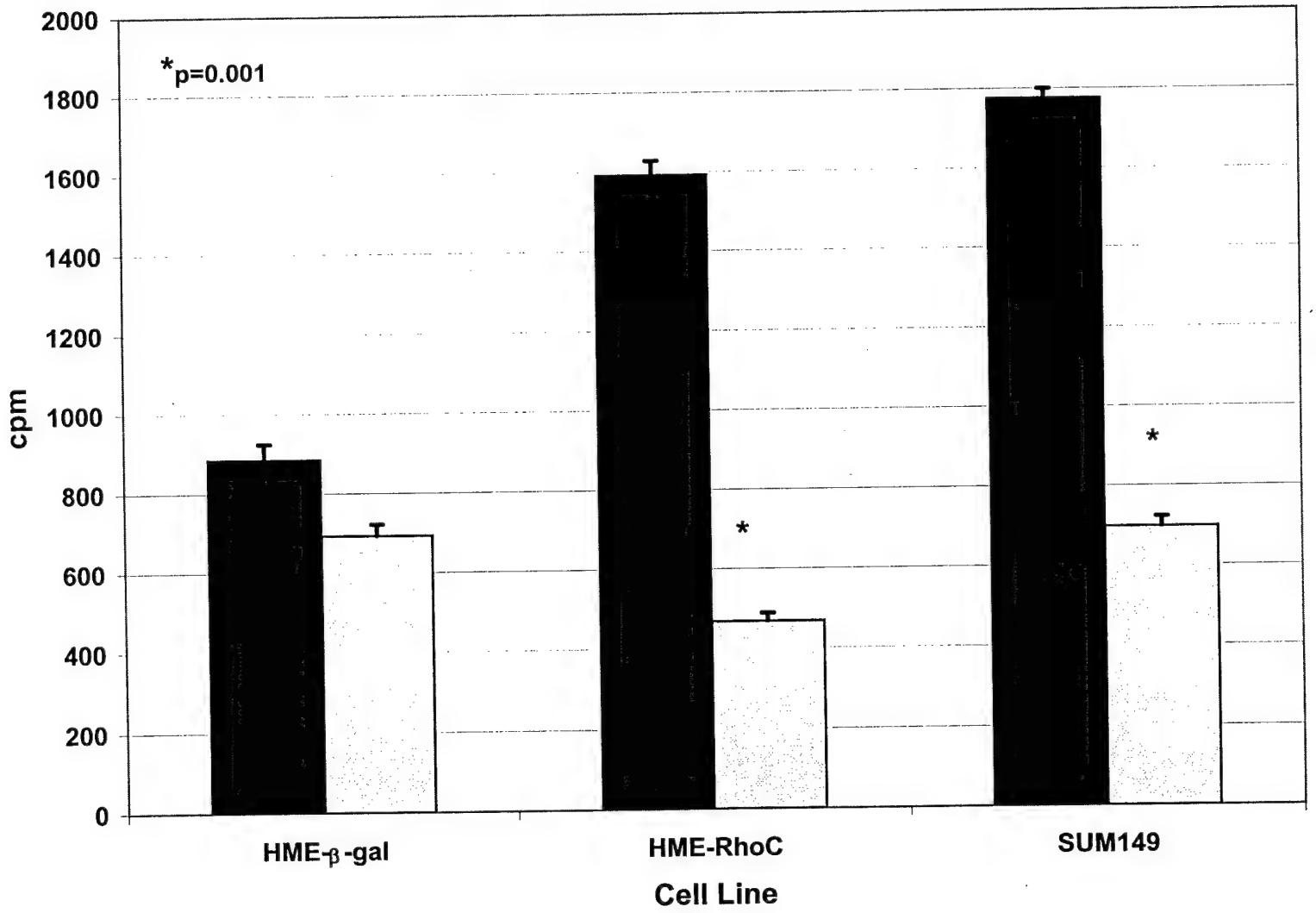
2000
1800
1600
1400
1200
1000
800
600
400
200
0
cpm
*p=0.001
*
*
HME-β-gal
HME-RhoC
SUM149
Cell Line

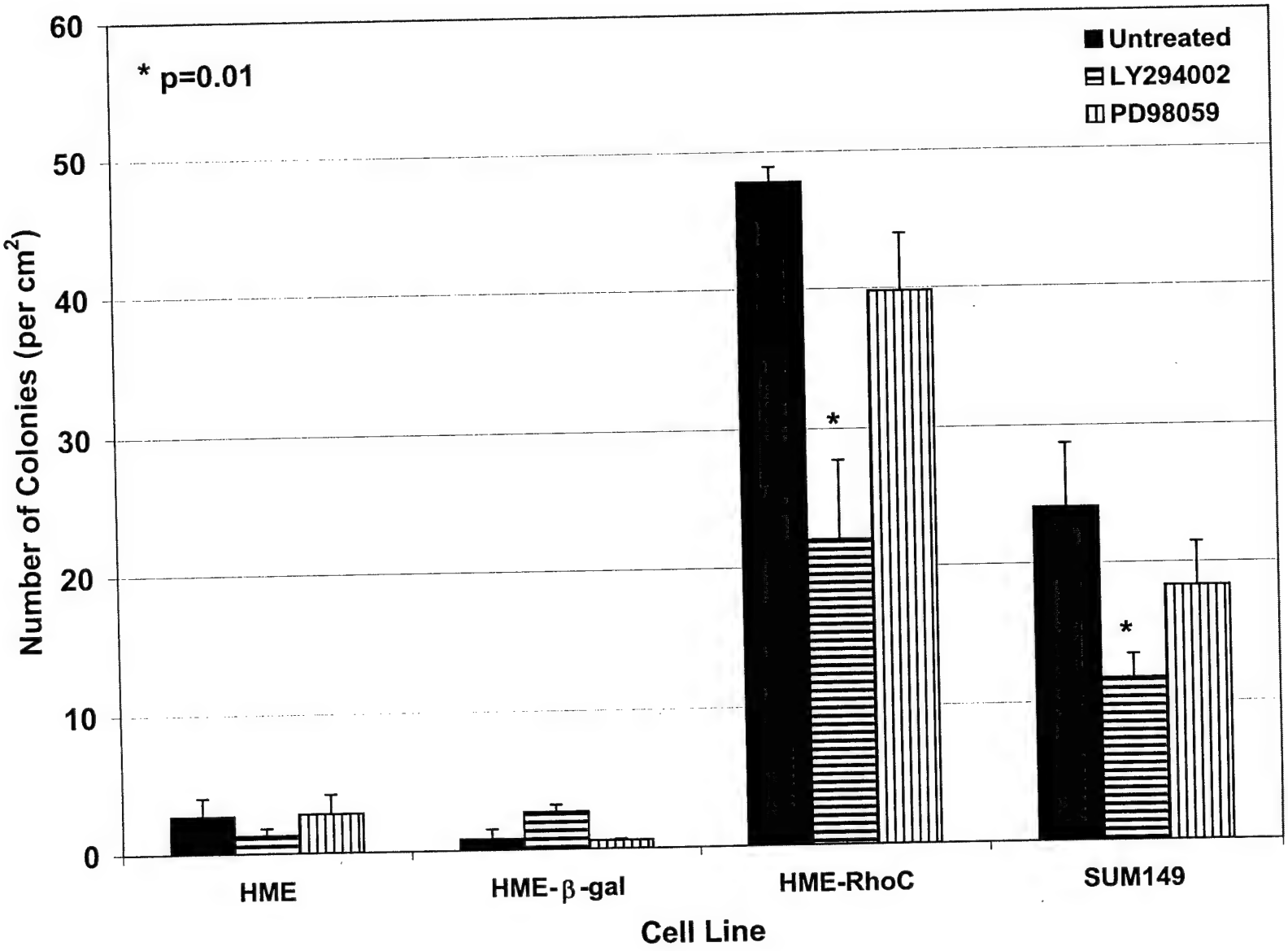
* p=0.01
Untreated
LY294002
PD98059
Number of Colonies (per cm2)
60
50
40
30
20
10
0
*
*
HME
HME-β-gal
HME-RhoC
SUM149
Cell Line

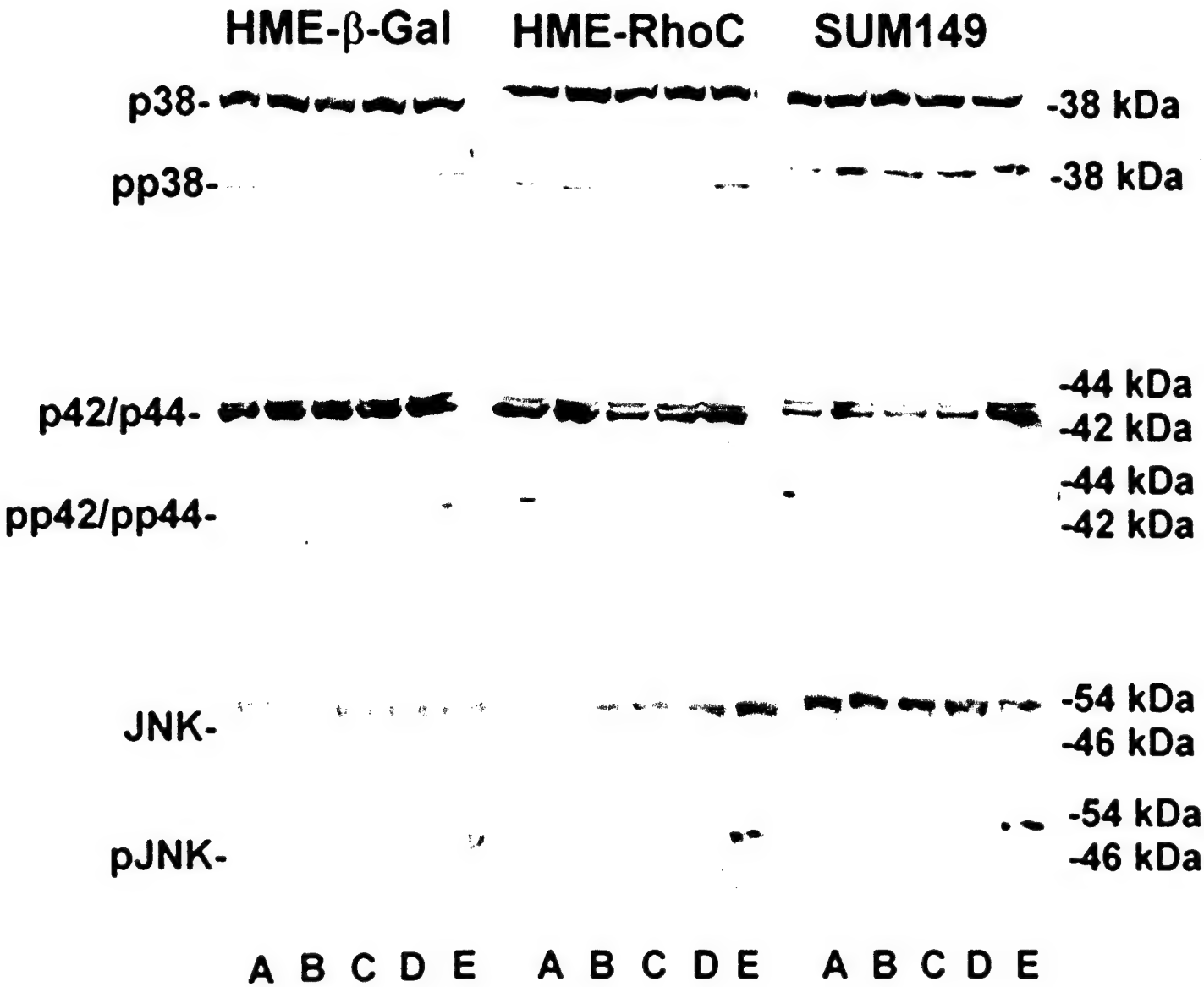
HME-β-Gal
HME-RhoC
SUM149
p38-
-38 kDa
pp38-
-38 kDa
p42/p44-
-44 kDa
-42 kDa
pp42/pp44-
-44 kDa
-42 kDa
JNK-
-54 kDa
-46 kDa
pJNK-
-54 kDa
-46 kDa
A B C D E A B C D E A B C D E

A

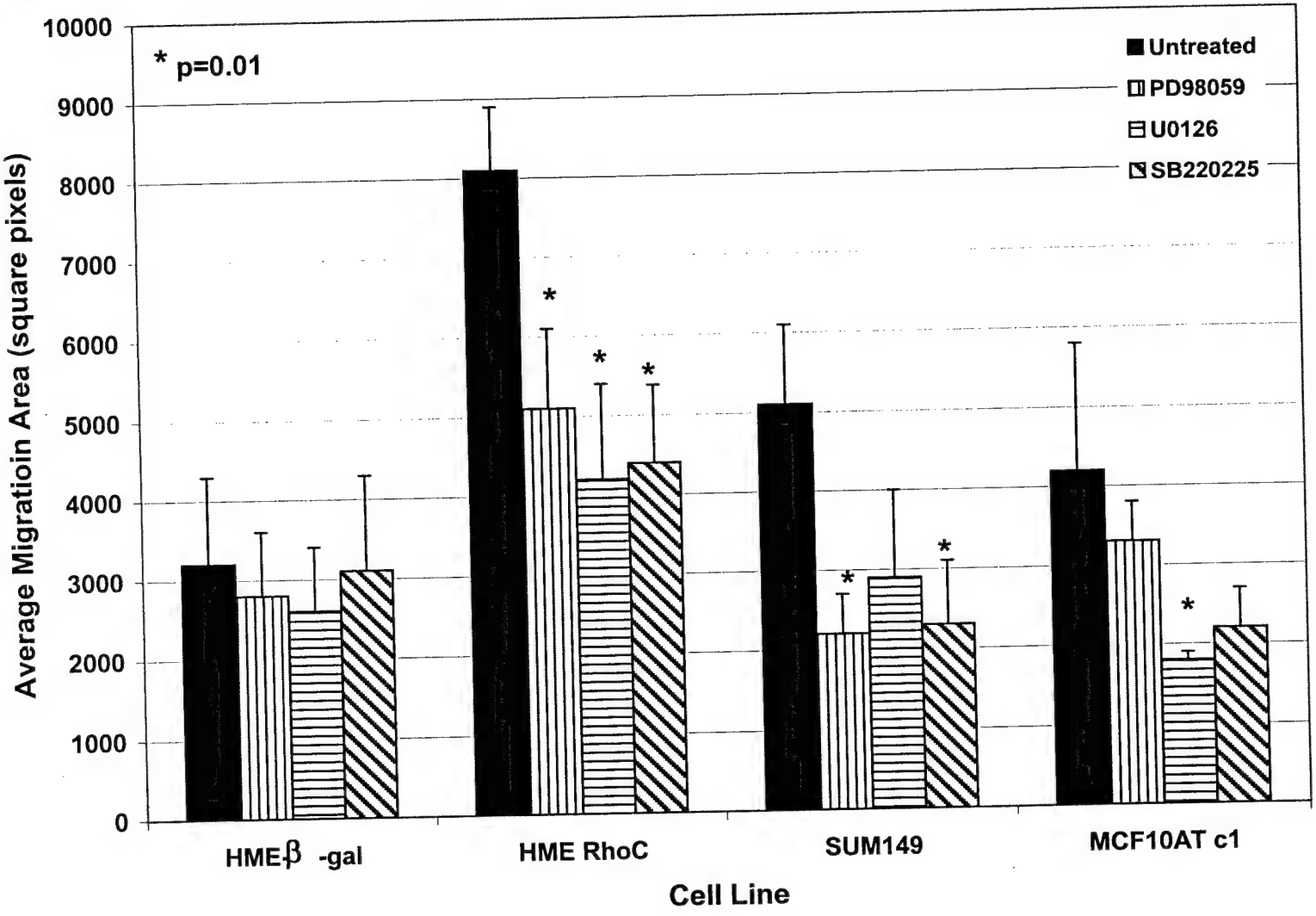
* p=0.01
Untreated
PD98059
U0126
SB220225
Average Migratioin Area (square pixels)
10000
9000
8000
7000
6000
5000
4000
3000
2000
1000
0
HMEβ -gal
HME RhoC
SUM149
MCF10AT c1
Cell Line

B

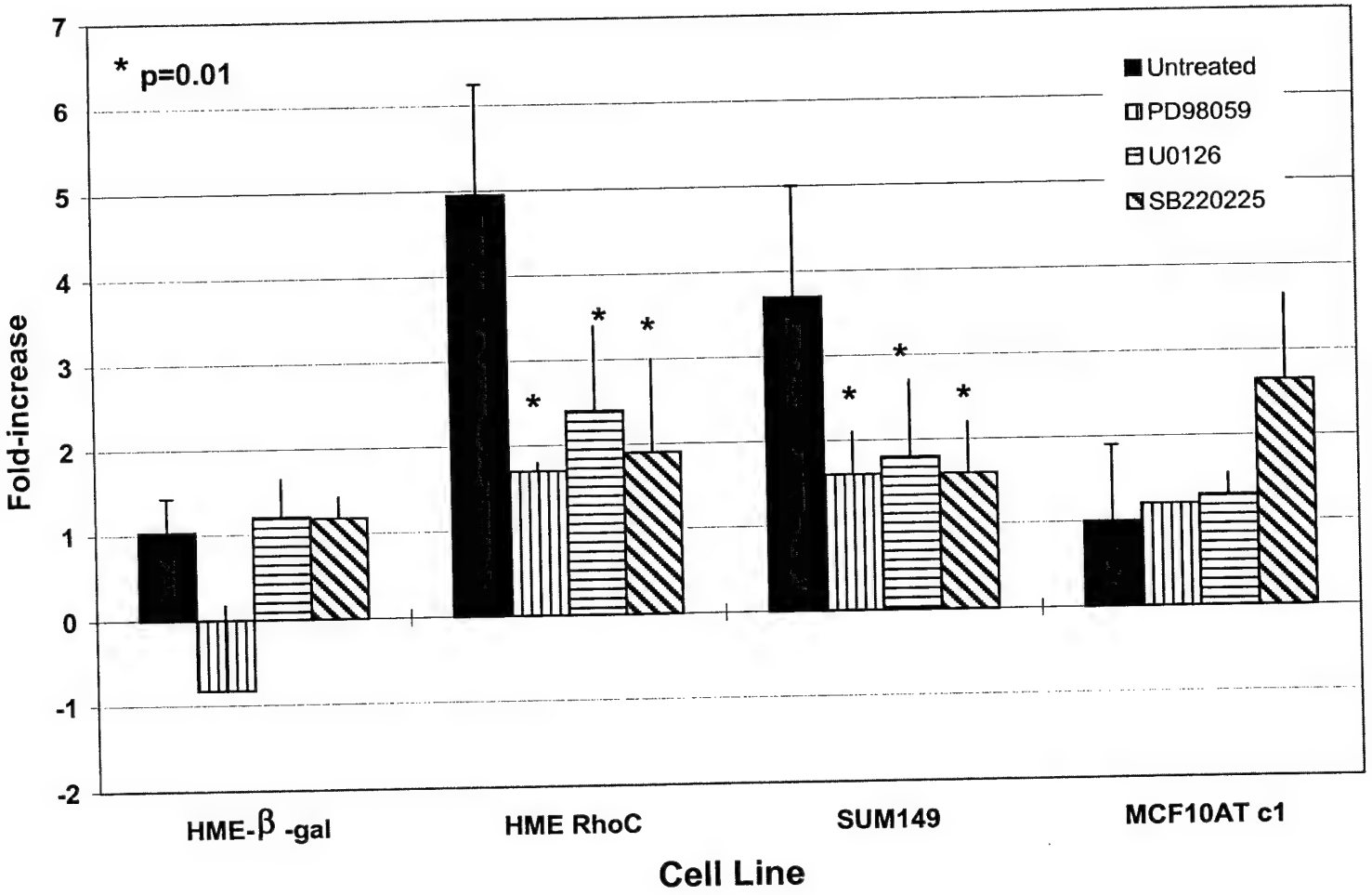
* p=0.01
Untreated
PD98059
U0126
SB220225
Fold-increase
7
6
5
4
3
2
1
0
-1
-2
HME-β -gal
HME RhoC
SUM149
MCF10AT c1
Cell Line

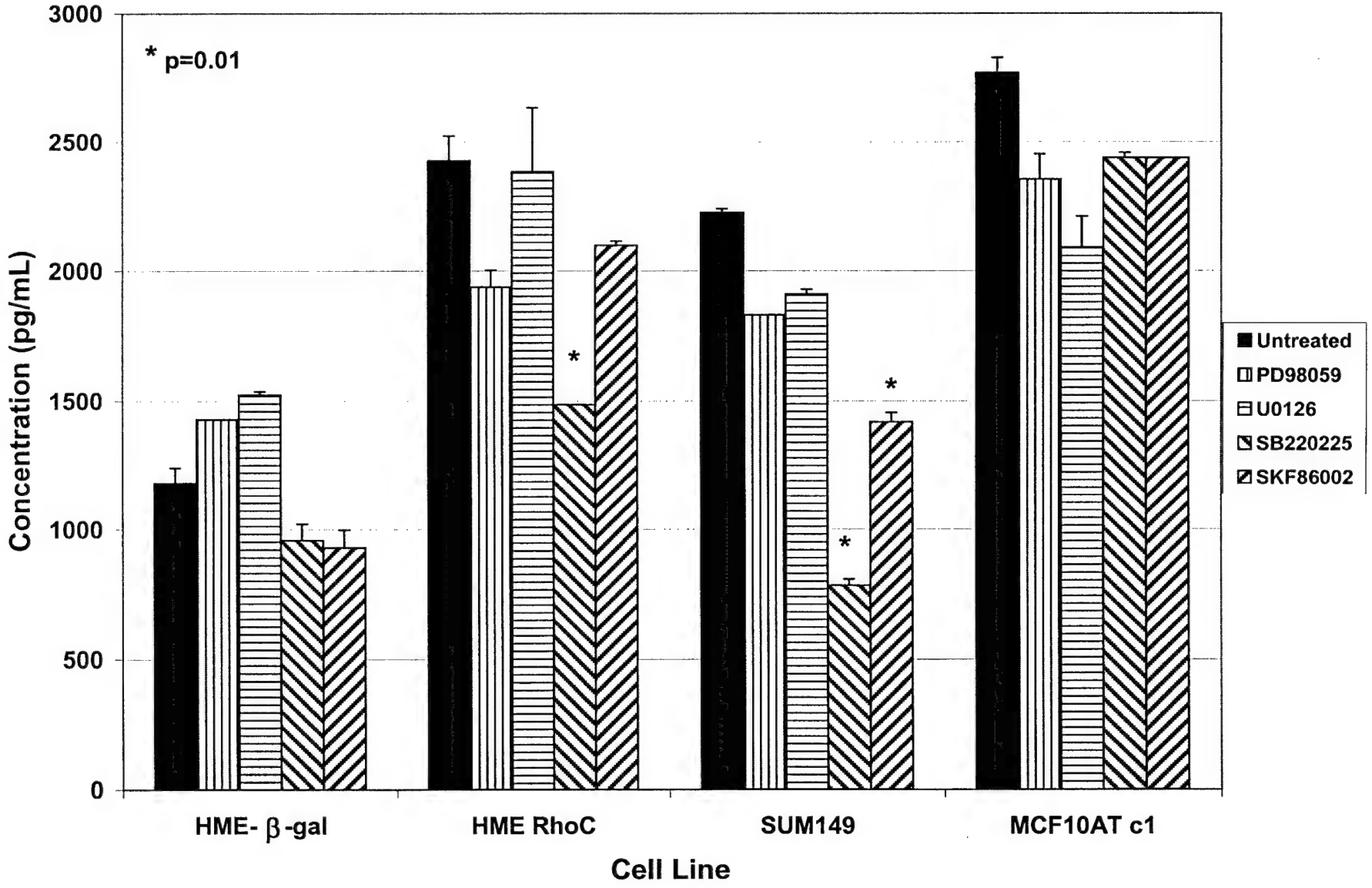
* p=0.01
3000
2500
2000
1500
1000
500
0
Concentration (pg/mL)
*
*
*
Untreated
PD98059
U0126
SB220225
SKF86002
HME- β-gal
HME RhoC
SUM149
MCF10AT c1
Cell Line

WISP3 Is a Novel Angiogenesis Inhibitor and Tumor Suppressor Gene of Inflammatory Breast Cancer

Celina G. Kleer[1*], M.D. Yanhong Zhang[1], M.D.,

Quintin Pan[2], Ph.D., Kenneth L. van Golen[2], Ph.D., Zhi-Fen Wu[2], M.D., Donna Livant[2,3],

and Sofia D. Merajver[2], M.D., Ph.D

Departments of Pathology (1), Internal Medicine, Division of Hematology and Oncology (2), Department of Radiation Oncology (3) and the University of Michigan Comprehensive Cancer Center (1,2,3), Ann Arbor, Michigan.

*To Whom Correspondence Should Be Addressed: 2G332 University Hospital, Department of Pathology. University of Michigan Medical School, 1500 East Medical Center Drive, Ann Arbor, MI 48109-0054; e-mail: kleer@umich.edu

Work supported in part by DOD grant DAMD17-00-1-0636 (CGK), NIH grants RO1CA77612 (SDM), P30CA46592, M01-RR00042, and AI-19192 (EAM), American Cancer Society RPG-99-207-01-MBC (EAM), FDA FD-U-000505 (GJB), and the Tempting Tables Organization, Muskegon, MI.

Text length: 38,134 characters including spaces.
Running title: WISP3 suppresses tumor angiogenesis and growth of human breast cancer.

ABSTRACT

Inflammatory breast cancer (IBC) is an aggressive form of breast cancer with a 5-year disease-free survival of less than 45%. Little is known about the genetic alterations that result in IBC. In our previous work, we found that WISP3 was specifically lost in human IBC tumors when compared to stage-matched, non-IBC tumors. We hypothesize that WISP3 has tumor suppressor function in the breast and that it may be a key genetic alteration that contributes to the unique IBC phenotype. The full-length WISP3 cDNA was sequenced and cloned into an expression vector. The resulting construct was introduced into the SUM149 cell line that was derived from a patient with IBC and lacks WISP3 expression. In soft agar assays, stable WISP3 transfectants formed significantly fewer colonies than the controls. Stable WISP3 transfectants lost their ability to invade and had reduced angiogenic potential. WISP3 transfection was effective in suppressing *in vivo* tumor growth in nude mice. Mice bearing WISP3 expressing tumors had a significantly longer survival than those with vector-control transfectant tumors. Our data demonstrate that WISP3 acts as a tumor suppressor gene in the breast. Loss of WISP3 expression contributes to the phenotype of IBC by regulating tumor cell growth, invasion and angiogenesis.

INTRODUCTION

Inflammatory breast cancer (IBC) is the most lethal form of locally advanced breast cancer and accounts for approximately 6% of new breast cancer cases annually in the United States (1,2). It is also a very distinct clinical and pathological form of breast carcinoma. It is characterized clinically by erythema, skin nodules, dimpling of the skin (termed "peau d'orange") and by a very rapid onset of disease, typically progressing within 6 months (1-4). Pathologically, carcinomatous tumor emboli spread through the dermal lymphatics which are responsible for the clinical signs and symptoms (2). IBC is generally not associated with precursor lesions (1,2). From the outset, IBC is highly invasive and it appears to be capable of metastases from its inception. It is estimated that nearly all women with IBC have nodal involvement at the time of diagnosis, and over one third have distant metastases (3,4). In spite of new advances in breast cancer therapy, the overall 5-year disease-free survival rate is less than 45% (3,4).

The genetic alterations underlying the development and progression of IBC were unknown until recently. Our laboratory identified two genes that are consistently and concordantly altered in human IBC when compared to stage-matched, non-IBC tumors: loss of WISP3 and over-expression of RhoC-GTPase (5).

WISP3 has been identified as a member of the CCN family of proteins, which have important biological functions in normal physiology as well as in carcinogenesis (6). There are only two publications in the literature on the biological effects of WISP3 and very little is known about the expression pattern and function of this novel gene (7,8). We hypothesize that WISP3 may function as a growth-suppressing factor in breast carcinogenesis and that it may be a key genetic alteration in IBC in particular. To test this

hypothesis, we set out to determine whether restoring WISP3 expression in an IBC cell line, SUM149, could abrogate or modulate the highly malignant IBC phenotype. We observed that stably transfected SUM149/WISP3 cells exhibited a striking decrease in proliferation rate, anchorage independent growth, invasion, and tumor growth in nude mice compared to empty vector transfectants. This work suggests new insights into the role of WISP3 in carcinogenesis in general.

MATERIALS AND METHODS

Cell culture

The derivation of the SUM149 cell line has been described previously by Ethier et al (9). This cell line was developed from a human primary inflammatory breast cancer and has lost WISP3 expression (Figure 1, lane F). Cells were cultured in Ham's F-12 medium supplemented with 5% FBS, hydrocortisone (1 μg/ml), insulin (5 μg/ml), fungizone (2.5 μg/ml), Gentamycin (5 μg/ml) and each of Penicillin/streptomycin (100 μ/ml) at 37G under 10% CO_2.

Construction of Expression Vector and Transfection

Total RNAs were isolated from human mammary epithelial cells (HME) using a Trizol kit (Life Technologies, Inc., Gaithersburg, MD). First–strand cDNA synthesis was performed using 1 μg of total RNA with AMV reverse transcriptase (Promega, Madison,WI) and oligo (dT) as a primer. Two μl of the reaction mixture were used for PCR amplification. Human WISP3 cDNA was amplified by PCR using the following forward and reverse primers: 5'-ATGCAGGGGCTCCTCTTCTGC-3' and 5'-ACTTTTCCCCCATTTGCTTG-3', under the following conditions: denaturing for 1 min at 94°C, annealing for 1 min at 58°C, and elongation for 2 min at 72°C for 35 cycles. The PCR product was cloned into pGEM-T Easy vector (Promega, Madison,WI). The 1.1kb full-length cDNA encoding WISP3 was excised by EcoRI and subcloned into the EcoRI site of pFLAG-CMV4 vector (Sigma, Saint Louis, Missouri). The insert was confirmed by DNA sequencing. The plasmids were purified. Subsequently, the SUM149 cells were transfected with pFlag-WISP3 and pFlag control vector by FuGene TM 6 transfection

reagent (Roch-Boehringer Mannheim, Mannheim. Germany), and selected in the medium containing 150 μg/ml G418. The cells surviving during selection were expanded and maintained in the selected medium.

Western Immunoblots

Western immunoblots were performed using the following primary antibodies: WISP3 polyclonal antibody, $p27^{kip1}$, $p21^{waf1}$, PCNA (Zymed, San Francisco, CA), cyclin E (SC-247, Santa Cruz, CA), cyclin D1 (SC-246, Santa Cruz, CA), and actin (Sigma chemical Co.). Cells were lysed in RIPA buffer (1x PBS, 1% Nonidet P-40, 0.5% sodium deoxycholate, 0.1% SDS, 0.1 mg/ml PMSF, 1mM sodium orthovanadate, and 0.3 mg/ml aprotinin; Sigma Chemical Co.). Whole cell lysates (50 μg) were boiled in Laemelli buffer for 5 minutes, separated by 10% SDS-PAGE and transferred to PVDF membrane. Non-specific binding was blocked by incubation with 1.5% BSA in Tris-buffered saline with 0.05% Tween-20 (Sigma Chemical Co.). Antibody-antigen complexes were detected with an enhanced chemiluminescence kit (ECL, Amersham, Arlington Heights, Ill.) following the manufacture's instructions.

Anchorage-independent Growth

Cells were seeded at a density of 1 x 10^3 per 35-mm plate in 0.3% agar and Ham's F-12 supplemented with 10% FBS, and plated on a base of 0.6 % agar, Ham's F-12 and 10 % FBS. Each assay was performed in triplicate. Plates were maintained at 37°C under

10% CO_2 for 3 weeks. Colonies greater than or equal to 100 μm in diameter were counted.

Annexin V-FITC Binding Assay

SUM149/WISP3 H and L cells, and SUM149/Flag control cells (1 x 10^6) were tripsinized, washed and incubated in binding buffer (10 nM HEPES/NaOH, 140 nM NaCl, 2 nM CaCl) containing 1 μg/ml of Annexin V-FITC conjugate (Clontech, CA) for 10 minutes in the dark. Cells were next stained with propidium iodide (20 μg/ml) and analyzed by flow cytometry.

Monolayer Growth Rate

Monolayer culture growth rate was determined by qualitative measurement of the conversion of MTT (3-(4,5-Dimethylthiazol-2-yl)-2,5-diphenyltetrazolium bromide, Sigma Chemical Co.) to a water insoluble formazan by viable cells. Three thousand cells in 200μl of culture medium were plated in 96-well plates and grown under normal conditions. Cultures were assayed at 0,1,3,4 and 5 days by the addition of MTT and incubation for 1 hour at 37°C. The MTT containing medium was aspirated and 100 μl DMSO (Sigma Chemical Co.) was added to lyse the cells and solubilize the formazan. Absorbance values of the lysates were determined on a Dynatech MR 5000 microplate reader at 540 nm.

Anchorage-independent Growth.

For studies of anchorage-independent growth of SUM149/FLAG and SUM149/WISP3, each well of a 6-well plate was first layered with 0.6% agar diluted

with 10% FBS supplemented Ham's F-12 medium complete with growth factors. The cell layer was then prepared by diluting agarose at concentrations of 0.3% and 0.6% with 10^3 cells in 2.5% FBS supplemented Ham's F-12/1.5 ml/well. Plates were maintained at 37°C under 10% CO_2 for 3 weeks. Colonies greater than or equal to 100 μm in diameter were counted.

Invasion and Intravasation

To study invasion, the sea urchin extracellular membrane (SU-ECM) invasion assay was used (10). Cells were layered onto sea urchin embryo extracellular basement membrane and allowed to invade for 4 hours. The cells on the SU-ECM were fixed using paraformaldehyde and visualized under a microscope. Mean invasion percentages were calculated from 2 independent analysis of 50-100 random cells.

Angiogenesis and Angiogenic Factor Analysis

To study whether WISP3 modulates the angiogenic activity of IBC, the levels of key pro-angiogenic factors known to be secreted by IBC (VEGF, FGF2, IL-6, and IL-8) were measured in the cell culture supernatants by ELISA (11). A functional analysis of angiogenesis of the conditioned media was performed. We used the rat aortic assay in which we assessed the amount of new blood vessel growth elicited by the conditioned medium of the WISP3 transfected cells (12). Approximately 1-mm thick rings were cut from the aorta of a freshly sacrificed rat and embedded into Matrigel in the center of a 35-mm dish. Vessel outgrowth from the aorta into the Matrigel was visually quantitated under a light microscope and compared at 7 and 10 days after plating.

In Vivo Tumor Formation

Groups of 5-11, 10-week old, nude, athymic female mice were orthotopically injected into the mammary fat pad with 2 x 10^6 cells. Each group was injected with either a control (SUM149/Flag, or wild-type SUM149) clone, one high WISP3-expressing clone (H), or a low WISP3-expressing clone (L). The clones were selected according to the WISP3 expression by RT-PCR and their anchorage-independent growth characteristics. Mice were then monitored weekly for tumor formation for 8 weeks and for signs of wasting and chachexia as surrogates of survival for 18 weeks. If tumors were present, tumor volume was calculated using the formula ($l \times w^2$)/2 (were l = length and w = width of tumor). Rates of tumor formation were analyzed by the Kruskal-Wallis method; tumor volumes were assessed between the groups by the Mann-Whitney U test; and the Kaplan Meier analysis was performed to evaluate survival. After the mice developed signs and symptoms of chachexia, they were sacrificed and their tumors were removed. A portion of each tumor (1/3) was digested with 0.1% collagenase (Type I) and 50 ug/ml DNase (Worthington Biochemical Corp. Freehold, NJ), and RNA was collected for RT-PCR analysis. The remainder of the tumor tissues were used for histolopathological study. After removal of the tumors, part of the tissues were fixed in 10% buffered formalin and processed for histopathological evaluation by paraffin-embedding and hematoxylin and eosin staining. Histological features studied included degree of anaplasia, mitotic activity, presence and amount of necrosis, and degree of differentiation (e.g. glandular formation).

RESULTS

Transfection with the SUM149 cell line with WISP3 cDNA

Figure 1 shows the Western blot analysis of WISP3 protein in whole cell lysates from 4 clones of SUM149/WISP3 stable transfectants, SUM149/Flag (transfection controls), SUM149 wild type, and HME cells. We used a specific anti-WISP3 antibody (gift from Dr. Mathew Warman). For subsequent experiments we will employ SUM149/WISP3 clones with a range of well-characterized WISP3 expression.

WISP3 induces a striking morphologic change in IBC cell line

After stable transfection with SUM149/WISP3 H and L clones and SUM149/Flag control we observed marked morphologic differences (Figure 2 A). Whereas the control SUM149/Flag cells had a characteristic tightly packed, cobblestone appearance, with a cuboidal shape and high nuclear to cytoplasmic ratio, the SUM149/WISP3 transfectants were heterogeneous in size and morphology. They became large, round, and flat with abundant granular and vacuolated cytoplasm and ill-defined cell borders. A detailed ultrastructural analysis by electron microscopy demonstrated that the WISP3 transfectants exhibited numerous cytoplasmic lysosomal bodies surrounded by a membrane, some containing electron-dense material and invaginated and convoluted nuclei (Figure 2b). These morphologic features have been described in cells undergoing senescence (13,14).

WISP3 partially abrogates angiogenesis in IBC

As illustrated in Figure 3a, SUM149/WISP3 clones produce significantly decreased levels of FGF2 (bFGF) and VEGF, key pro-angiogenic factors. In addition, the levels of IL-6 were significantly decreased. To investigate whether the decreased production of angiogenic factors induced by restoration of WISP3 expression resulted in the inhibition of neovascularization, we carried out rat aortic ring assays. After 10 days of incubating a rat aortic ring with the cell culture supernatant, fewer vessels were formed by SUM149/WISP3 cells when compared to the controls (Figure 3b). These results show that expression of WISP3 depressed the strength of the tumor-induced signal for angiogenesis.

Expression of WISP3 reduces the proliferation rate, anchorage-independent growth, and the invasive ability of IBC cells

Figure 4a shows that the proliferation rate of the SUM149 cell line transfected with WISP3 decreased significantly when compared to controls. No significant differences in proliferation rate were detected between the high and low WISP3 expressing clones.

As anchorage independent growth is a hallmark of malignant transformation, we investigated whether expression of WISP3 in highly malignant SUM149 cell line abolished this feature. After 14 days of growth in soft agar both the high and low WISP3 expressing clones formed significantly fewer and smaller colonies than the control cells (Figure 4b).

The ability of the transfectants to invade and intravasate was studied using the sea urchin extracellular membrane (SU-ECM) invasion assay. This assay provides a uniform biological, serum-free, basement membrane that closely mimics the type of extracellular matrix that cells encounter in vivo. Transfection with WISP3 completely abolished the ability of the IBC cells to invade, compared to the empty vector transfectant (Figure 4c). As was the case in the proliferation rates and anchorage-independent growth characteristics, no statistically significant differences in invasion were noted between the high and low WISP3 expressing clones.

WISP3 expression inhibits cellular growth by inducing accumulation of $p27^{kip1}$ and $p21^{waf1}$ in cancer cells and induces apoptosis.

Based on the morphologic changes of cellular senescence induced by transfection with WISP3, we set out to investigate whether WISP3 caused alterations in the regulation of the cell cycle, that could in turn be contributing to the inhibition of cellular proliferation, anchorage-independent growth, and in vivo tumor growth. To elucidate the possible effect of WISP3 on the cell cycle regulators, the round and vacuolated cells (SUM149/WISP3) were assayed for the presence of several key cell cycle regulators by Western immunoblots. Interestingly, when compared to the control cells, the level of $p27^{kip1}$ and $p21^{waf1}$ were increased in the WISP3 transfectants (Figure 4d). Concordantly, SUM149/WISP3 exhibited decreased levels of cyclin E and PCNA, a reliable marker for cellular proliferation (Figure 5).

The percentage of apoptotic cells was significantly increased by WISP3 expression as detected by the Annexin V assay by flow cytometry. SUM149/WISP3

transfectants had 30% apoptotic cells when compared to SUM149/Flag control cell line with only 13% apoptotic cells.

WISP3 inhibits *in vivo* tumor growth and improves survival of mice

Given that WISP3 affects cell cycle regulation, proliferation rates and anchorage independent growth, we investigated the effect of restoration of WISP3 expression on SUM149 xenograft tumor growth and survival of the host mice. Three groups of 10-11 mice were injected with SUM149/WISP3 L, SUM149/WISP3 H, and a control group (SUM149/Flag and SUM149 wild type, 5 mice each). Mice with orthotopically implanted tumor cells were monitored weekly for tumor formation over an 8-week period. By the 8^{th} and final week of the experiment, palpable tumors developed in all mice that received injection of the SUM149/WISP3 L clone, in 10 of 11 mice that received injection of the SUM149/WISP3 H clone, and in 9 of 10 mice given injection of control clones (5 injected with SUM149-FLAG, and 5 injected with wild-type SUM149). The rate of tumor formation between WISP3 transfectants and controls differed (Table 1). Specifically, the clones transfected with WISP3 formed tumors at a slower rate than the controls ($p=0.05$). Moreover, when tumor volume was compared at each week (starting at week 2), it was significantly lower in the tumors formed by SUM149/WISP3 transfectants than in the tumors formed by the controls ($p=0.05$). When the slopes of the regression lines were compared, striking differences were found between the WISP3 transfectants and control cells ($p<0.001$, Figures 5a and 5b). At week 5, two tumors from each clone, and from the control were excised. WISP3 mRNA expression was confirmed by quantitative RT-PCR. Levels of WISP3 expression were found to be similar to those

of preinjection. Taken together, these results demonstrate that tumors formed by SUM149/WISP3 take longer to grow and are smaller than controls.

To address whether the tumors formed by the transfectants expressing WISP3 were pathologically different from the control, histopathologic study of the tumors was carried out. As shown in Figure 5a, SUM149/Flag tumors were highly anaplastic, had strikingly atypical cells forming solid aggregates, with no glandular formation, a sign of poor differentiation, and extensive areas of necrosis. The cells exhibited high mitotic activity (mean 88 mitoses per 10 high power field) and numerous abnormal mitoses. In contrast, the tumors derived from SUM149/WISP3 clones had less nuclear pleomorphism and slightly better differentiation evidenced by occasional gland formation. These tumors had less necrosis and the mitotic activity was greatly decreased (mean 11 mitoses per 10 high power fields). The mice injected with the high WISP3 expressing cells (SUM149/WISP3 (H)) had a significantly better survival than the controls and the low WISP3 expressing cells (SUM149/WISP3 (L)) ($p=0.02$, Wilcoxon log-rank test. Figure 5c).

DISCUSSION

WISP3 is located in chromosome 6q21-22 and encodes for a 54 amino acid, 36.9 kDa protein with the modular architecture of the CCN family of proteins which includes connective tissue growth factor (CTGF), Cyr61, Nov, WISP1 and WISP2 (6-8,15-20). The CCN proteins participate in fundamental biological processes such as cell proliferation, migration, wound healing, angiogenesis and tumorigenesis (6). They have a range of biological properties that might be dependent upon the cellular context (6).

In tumorigenesis, Cyr61 and WISP1 were reported to act as positive regulators of cell growth (7,15-20); Nov expression was found to correlate with the development of metastases in Ewing's sarcomas, prostate cancer, and renal cell carcinomas (6), whereas it was found to act as a negative growth regulator of glioblastoma cell lines (21). Furthermore, in primary human colonic adenocarcinomas, the expression of WISP2 was significantly decreased compared to normal colon (8), and it was not detected in the epithelial tumor cells of mammary carcinoma obained from Wnt-1 transgenic mice (8). Similarly, in our study we could not detect WISP3 mRNA expression in 80% of the IBC human tissues studied (5). The expression of ELM1/WISP1, which had been reported to suppress the metastatic potential of murine melanoma cells (16), was significantly increased in most human colonic carcinomas (8,20). These data provide compelling evidence that the CCN proteins may have opposing functions in carcinogenesis in different cell types and tissues.

There are only two previous publications in the literature on the biologic properties of WISP3 (7,8). In one of these studies, the WISP3 gene was significantly over-expressed in human colon carcinoma (7) whereas Hurvitz et al found loss of

function mutations in the WISP3 gene to be associated with progressive pseudorheumatoid dysplasia in humans (8). Patients with progressive pseudorheumatoid dysplasia due to WISP3 loss-of-function mutations have not been reported to have higher rates of cancer; however this has not been systematically sought in this cohort (8). Our data provide evidence that WISP3 has tumor suppressor function in the mammary gland.

Using a modified version of the differential display technique and in situ hybridization of human breast cancer tissues, we found that WISP3 is lost in 80% of IBC and in 21% of stage matched, non IBC tumors ($p=0.0013$, Fisher's exact test) (5). WISP3 loss was found in concert with RhoC-GTPase over-expression in 90% of archival IBC patient samples, but not in stage-matched non-IBC tumors (5). Our laboratory demonstrated that RhoC-GTPase over-expression produces a motile and invasive phenotype in human mammary epithelial cells, primarily through formation of actin stress fibers and focal adhesion points (22). We hypothesized that loss of expression of WISP3 contributes to the development of the IBC phenotype by altering angiogenesis and tumor growth, therefore complementing the role of RhoC-GTPase over-expression.

One of the features that define the IBC phenotype as unique is its rapid progression, with fast growth and invasion, making it the most lethal form of locally advanced breast cancer (1-4). IBC is characterized by a rapid onset of disease, typically arising within 6 months, and by the time of diagnosis, the majority of patients have locoregional and distant metastatic disease (1-4). Transfection of the IBC cell line SUM149 with WISP3 cDNA inhibited some of these key phenotypic characteristics.

The proliferation rate of highly aggressive SUM149 cell line was decreased, and growth under anchorage independent conditions was greatly reduced in the stable WISP3

transfectants. In comparison with the control cells, the WISP3 transfectants produced 6-16 -fold less colonies than the control cells. Similarly, the effect of transfection with WISP3 on cancer cell invasion was striking. Using the sea urchin invasion assay, a system that closely resembles the extracellular matrix that cells encounter in vivo, the WISP3 transfectants did not invade, when compared to controls. Furthermore, transfection with WISP3 cDNA greatly reduced tumor growth *in vivo.* Interestingly, transfection with WISP3 also resulted in a decrease in the rate of tumor uptake.

Another feature that makes IBC unique is its high angiogenic and angioinvasive potential. We proved that WISP3 suppressed pathologic neovascularization by reducing the levels of key pro-angiogenic factors, FGF2, VEGF, and IL-6.

Although the mechanism of action of the CCN proteins in general and of WISP3 in particular has not been elucidated, there are several candidates. The first of these could be by regulating nuclear cycling and/or apoptotic functions (23-24). We observed a marked morphologic change in the SUM149 cell line after transfection with WISP3 cDNA. Histopathologic study of the tumors developed in nude mice revealed that those derived from the WISP3 transfectants had a significant reduction in the mitotic activity, as well as better differentiation and less cellular and nuclear pleomorphism. To better understand these morphologic changes, we studied the levels of key cell cycle regulators and apoptosis. The levels of the cell cycle inhibitors $p27^{kip1}$ and $p21^{waf1}$ were markedly increased by WISP3 expression, and cyclin E was concordantly decreased. Consistent with these cell-cycle specific gene expression changes, the percentage of apoptotic cells was also increased in the WISP3 transfectants. These data suggest that in the mammary

gland, WISP3 expression may inhibit cancer cell growth through modulation of the cell cycle regulation and apoptosis.

A second possible mode of tumor suppression activity for WISP3 is by regulating angiogenesis (6,15). As the tumor grows, it requires and promotes an increase in neovascularization. This activation of the angiogenic switch involves the up-regulation of angiogenic inducers and/or down-regulation of angiogenic inhibitors. Our results show that WISP3 expression induces a reduction in the level of key pro-angiogenic factors which results in a decrease in functional neovascularization.

A third mechanism of WISP3 tumor suppression could be by binding IGF-like ligands. WISP3 has the modular architecture of the CCN proteins and consists of four domains: an IGF-binding protein domain, a Von Willebrand factor domain, a thrombospondin 1 domain, and a C terminal domain (6-8,15,16). The N-terminal domain includes the first 12 cysteine residues and contains the highly conserved IGF binding consensus sequence (GCGCCXXC) which specifically binds IGF (25-26). The thrombospondin type 1 domain (TSP1) is presumably involved in inhibition of angiogenesis (6). The carboxy-terminal domain (CT) is present in all CCN proteins described to date and forms a cysteine knot. The protein is folded into two highly twisted antiparallel pairs of beta-strands and contains three disulfide bonds that may participate in dimerization and receptor binding. The CT domain does not appear to be as critical in IGF binding as the N-terminal region that contains the IGF-binding protein motif (25-26). Although WISP3 may function in tumorigenesis through modulation of IGF binding, this is less likely since IGF-binding activity could not be demonstrated for other members of the CCN family (6). We are currently investigating this possibility in mammary tissue.

In summary, we have proven that restoring expression of WISP3 into an aggressive IBC cell line, SUM149, inhibited cellular proliferation, drastically decreased angiogenesis, inhibited invasion, and decreased anchorage-independent growth, all hallmarks of malignant transformation. Restoration of WISP3 expression resulted in a morphologic alteration and induced tumor cell apoptosis with concordant molecular changes in cell cycle specific genes, $p27^{kip1}$ and $p21^{waf1}$. Finally, when SUM149 cells transfected with WISP3 were injected into female athymic nude mice, the rate of tumor formation and the tumor volume were markedly decreased when compared to controls. These data demonstrate for the first time that WISP3 has strong tumor suppressor function in the mammary gland. Given the seemingly specific role that WISP3 plays in the development of IBC, our work may lead to the development of novel therapies that replace or mimic WISP3 function to treat this particularly challenging form of breast cancer.

REFERENCES

1. Jaiyesimi,I., Buzdar,A., and Hortobagyi,G. 1992 Inflammatory Breast Cancer: A Review. *J Clin Oncol*, 10 , 1014-1024.
2. Lee,B.J. and Tannenbaum,N.E. 1924 Inflammatory carcinoma of the breast: A report of Twenty-eight cases from the breast clinic of Memorial Hospital. *Surg Gynecol Obstet*, 39, 580-595.
3. Merajver SD, Weber BL, Cody R, Zhang D, Strawderman M, Calzone KA, LeClaire V, Levin A, Irani J, Halvie M, August D, Wicha M, Lichter A, Pierce L. 1997. Breast conservation and prolonged chemotherapy for locally advanced breast cancer: The University of Michigan experience. J Clin Oncol 15(8):2873-2881.
4. Swain SM, Sorace RA, Bagley CS, Danforth DN Jr, Bader J, Wesley MN, Steinberg SM, Lippman ME. 1987 Neoadjuvant chemotherapy in the combined modality approach of locally advanced nonmetastatic breast cancer. Cancer Res 15;47(14):3889-94.
5. van Golen,K.L., Davies,S., Wu,Z.F., Wang,Y., Bucana,C.D., Root,H., Chandrasekharappa,S., Strawderman,M., Ethier,S.P., and Merajver,S.D. 1999 A novel putative low-affinity insulin-like growth factor-binding protein, LIBC (lost in inflammatory breast cancer), and RhoC GTPase correlate with the inflammatory breast cancer phenotype. *Clin Cancer Res*, 5, 2511-2519.
6. Perbal B. 2001 NOV (nephroblastoma overexpressed) and the CCN family of genes: structural and functional issues. Mol Pathol. 54(2):57-79. Review.
7. Pennica,D., Swanson,T.A., Welsh,J.W., Roy,M.A., Lawrence,D.A., Lee,J., Brush,J., Taneyhill,L.A., Deuel,B., Lew,M., Watanabe,C., Cohen,R.L., Melhem,M.F., Finley,G.G., Quirke,P., Goddard,A.D., Hillan,K.J., Gurney,A.L.,

Botstein,D., and Levine,A.J. 1998 WISP genes are members of the connective tissue growth factor family that are up-regulated in Wnt-1-transformed cells and abberrantly expressed in human colon tumors. *Proc.Natl.Acad.Sci USA*, 95, 14717-14722.

8. Hurvitz JR, Suwairi WM, Van Hul W, El-Shanti H, Superti-Furga A, Roudier J, Holderbaum D, Pauli RM, Herd JK, Van Hul EV, Rezai-Delui H, Legius E, Le Merrer M, Al-Alami J, Bahabri SA, Warman ML. 1999 Mutations in the CCN gene family member WISP3 cause progressive pseudorheumatoid dysplasia Nat Genet. 23(1):94-8.
9. Ethier,S.P., Mahacek,M.L., Gullick,W.J., Frank,T.S., and Weber,B.L. 1993 Differential isolation of normal luminal mammary epithelial cells and breast cancer cells from primary and metastatic sites using selective media. *Cancer Res*, 53, 627-635.
10. Livant,D.L., Linn,S., Markwart,S., and Shuster,J. 1995 Invasion of a selectively permeable sea urchin embryo basement membranes by metastatic tumor cells, but not by their normal counterparts. *Cancer Res*, 55, 5085-5093.
11. van Golen KL, Wu ZF, Qiao XT, Bao L, Merajver SD. 2000 RhoC GTPase overexpression modulates induction of angiogenic factors in breast cells. Neoplasia. 2(5):418-25.
12. Nissanov,J., Tuman,R.W., Gruver,L.M., and Fortunato,J.M. 1995 Methods in Laboratory Investigation Automatic vessel sementation and quantification of the rat aortic ring assay of angiogenesis. *Lab Invest*, **73**, 734-739.

13. Romanov SR, Kozakiewicz BK, Holst CR, Stampfer MR, Haupt LM, Tisty TD. 2001 Normal human mammary epithelial cells spontaneously escape senescence and acquire genomic changes. Nature. 1;409(6820):633-7.

14. Tsugu A, Sakai K, Dirks PB, Jung S, Weksberg R, Fei YL, Mondal S, Ivanchuk S, Ackerley C, Hamel PA, Rutka JT. 2000 Expression of p57(KIP2) potently blocks the growth of human astrocytomas and induces cell senescence. Am J Pathol. 157(3):919-32.

15. Babic,A.M., Kireeva,M.L., Kolesnikova,T.V., and Lau,L.F. 1998 CYR61, a product of a growth factor-inducible immediate early gene, promotes angiogenesis and tumor growth. *Proc.Natl.Acad.Sci.U.S.A*, 95, 6355-6360.

16. Hashimoto Y, Shindo-Okada N, Tani M, Nagamachi Y, Takeuchi K, Shiroishi T, Toma H, Yokota J. 1998 Expression of the Elm1 gene, a novel gene of the CCN (connective tissue growth factor, Cyr61/Cef10, and neuroblastoma overexpressed gene) family, suppresses In vivo tumor growth and metastasis of K-1735 murine melanoma cells. J Exp Med. 187(3):289-96.

17. Kireeva ML, MO FE, Yang GP, Lau LF. 1996 Cyr61, a product of a growth factor-inducible immediate-early gene, promotes cell proliferation, migration, and adhesion. Mol Cell Biol. 16(4):1326-34.

18. O'Brien TP, Lau LF. 1992 Expression of the growth factor-inducible immediate early gene cyr61 correlates with chondrogenesis during mouse embryonic development. Cell Growth Differ. 3(9):645-54.

19. Wong M, Kireeva ML, Kolesnikova TV, Lau LF. 1997 Cyr61, product of a growth factor-inducible immediate-early gene, regulates chondrogenesis in mouse limb bud mesenchymal cells. Dev Biol. 192(2):492-508.

20. Xu L, Corcoran RB, Welsh JW, Pennica D, Levine AJ. 2000 WISP-1 is a Wnt-1- and beta-catenin-responsive oncogene. Genes Dev. 14(5):585-95.

21. Li WC, Martinerie C, Zumkeller W. 1996 Differential expression of novH and CTGF in human glioma cell lines. Mol Pathol;49:M91-7

22. van Golen KL, Wu Z, Qiao XT, Bao LW, Merajver SD. 2000. RhoC-GTPase, a novel transforming oncogene for human mammary epithelial cells that partially recapitulates the inflammatory breast cancer phenotype. Cancer Research 60:5832-5838.

23. Lopez-Bermejo A, Buckway CK, Devi GR, Hwa V, Plymate SR, Oh Y, Rosenfeld RG. 2000 Characterization of insulin-like growth factor-binding protein-related proteins (IGFBP-rPs) 1, 2, and 3 in human prostate epithelial cells: potential roles for IGFBP-rP1 and 2 in senescence of the prostatic epithelium. Endocrinology. 141(11):4072-80.

24. Sprenger CC, Damon SE, Hwa V, Rosenfeld RG, Plymate SR. 1999 Insulin-like growth factor binding protein-related protein 1 (IGFBP-rP1) is a potential tumor suppressor protein for prostate cancer. Cancer Res. 59(10):2370-5.

25. Imai Y, Moralez A, Andag U, Clarke JB, Busby WH Jr, Clemmons DR. 2000 Substitutions for hydrophobic amino acids in the N-terminal domains of IGFBP-3 and -5 markedly reduce IGF-I binding and alter their biologic actions. J Biol Chem. 275(24):18188-94.

26. Kim HS, Nagalla SR, Oh Y, Wilson E, Roberts CT Jr, Rosenfeld RG. 1997 Identification of a family of low-affinity insulin-like growth factor binding proteins (IGFBPs): characterization of connective tissue growth factor as a member of the IGFBP superfamily. Proc Natl Acad Sci U S A. 94(24):12981-6.

Acknowlegments

We thank Wendy Kutz and Matthew Warman from Case Western Reserve University for providing anti-WISP3 polyclonal antibody. We thank Satoru Hayasaka for excellent statistical support and Elizabeth Horn for artwork.

FIGURE LEGENDS

Figure 1. Western blot using a specific anti-WISP3 antibody demonstrates successful transfection and expression of WISP3 in SUM149 cells (lanes A-D). Lane E: transfection control (SUM149/Flag). Lane F: wild type SUM149. Lane G: HME cells with normal expression of WISP3.

Figure 2. ***a.*** Phase contrast microscopy showing the vacuolization and morphologic changes induced by restoring WISP3 expression in SUM149 cells. A: SUM149/Flag (controls). B: SUM149/WISP3 (X 200). ***b*** Electron microscopy. A. SUM149/Flag, and B. SUM149/WISP3 transfected cell showing a prominent intracytoplasmic dense vacuole.

Figure 3. ***a.*** Decrease in key angiogenic factors measured by ELISA, as a result of restoration of WISP3 expression in SUM149 cells. Results are expressed as mean ± SD. * $p<0.05$. ***b.*** Rat aortic ring assay showing marked decrease in new vessel formation from the pre-existing aortic ring bathed in conditioned media from SUM149/WISP3 cells (B), and SUM149/Flag controls (A). (100 X)

Figure 4. ***a.*** Effect of stable WISP3 transfection on the proliferation of SUM149 cells studied with the MTT assay. Results are expressed as mean ± SD of three independent experiments. 3,000 cells were assessed in each plate. ***b.*** Anchorage-independent growth in soft agar. Restoration of WISP3 in SUM149 cell line greatly decreased the number of the colonies formed. ***c.*** Restoration of WISP3 expression in SUM149 cell line abolished its invasiveness. Results are expressed as mean ± SD. ***d.*** Western immunoblot of cell

culture media of control (SUM149/FLAG), high and low WISP3 expressing clones using antibodies for p27kip1, p21waf1/cip1, cyclin E, and PCNA.

Figure 5. ***a top*** SUM149 cells transfected with WISP3 (A) formed smaller tumors than SUM149/Flag controls. Pictures were taken 5 weeks after injection (B). ***a bottom.*** Pathological features of the tumors. The tumors formed by SUM149/Flag controls are pleomorphic, with extensive necrosis and mitoses. The tumors formed by the SUM149/WISP3 clones are better differentiated, the cells are smaller, there is less necrosis and mitoses (hematoxylin & eosin stain, light microscopy, X400). ***b.*** Effect on tumor volume of restoration of WISP3 in SUM149 cells. When the slopes of the curves were compared, a significant difference was found between the transfectants and controls ($p<0.001$). No difference was detected between the high and low WISP3 expressing clones. Results are expressed as mean ± SEM. Wild type SUM149 were represented together with SUM149/FLAG because no statistically significant difference between the 2 groups was found. ***c.*** Kaplan Meier analysis of survival of mice injected with high and low WISP3 expressing clones compared to control clones. Wild type SUM149 are represented together with SUM149/Flag because no statistically significant difference between the 2 groups was found. Mice injected with the high WISP3 expressing clone had a significantly better survival than mice injected with the control clones (Log rank $p=0.02$). No differences were found between mice injected with the low WISP3 expressing clone and the control.

Table 1. Rate of tumor formation after orthotopic injection in the mammary fat pad of SUM149 wild type, SUM149/FLAG, high (SUM149/WISP3 H), and low (SUM149/WISP3 L) WISP3 expressing clones in female athymic nude mice. Tumors formed by the WISP3 transfectants tended to take a longer time to develop than tumors formed by the control cells (p=0.05).

	2 weeks n (%)	4 weeks n (%)	6 weeks n (%)	8 weeks n (%)
SUM149 wild type	5/5 (100)	5/5 (100)	5/5 (100)	5/5 (100)
SUM149/FLAG	4/5 (80)	4/5 (80)	4/4 (80)	4/5 (80)
SUM149/WISP3 H	9/11 (82)	10/11 (91)	10/11 (91)	10/11 (91)
SUM149/WISP3 L	3/10 (30)	5/10 (50)	9/10 (90)	10/10 (100)

FIG. 1

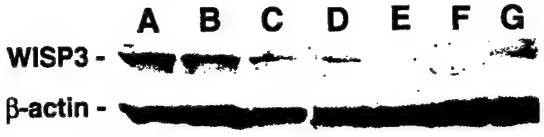

A - SUM149/WISP3 H1
B - SUM149/WISP3 H2
C - SUM149/WISP3 L1
D - SUM149/WISP3 L2
E - SUM149/FLAG
F - SUM149 WT
G - HME

Fig. 2.

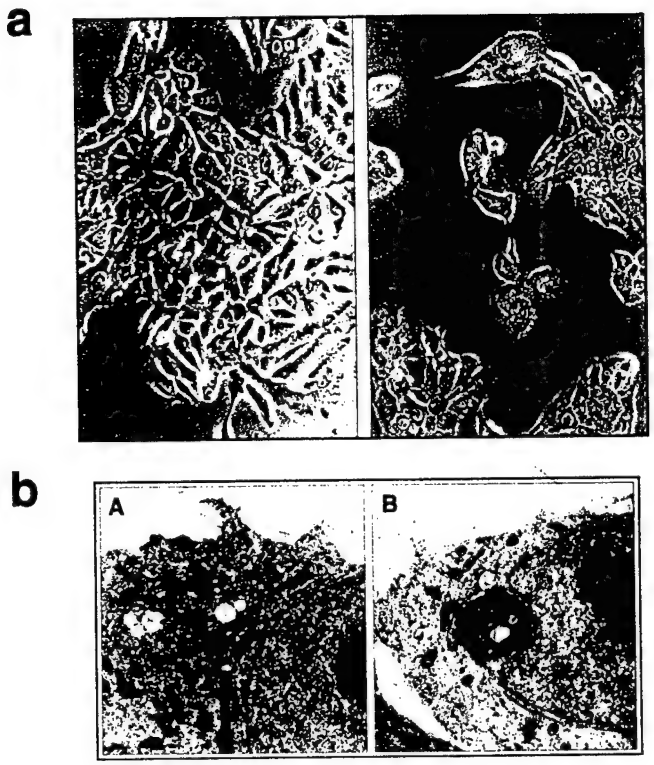

FIG. 3.

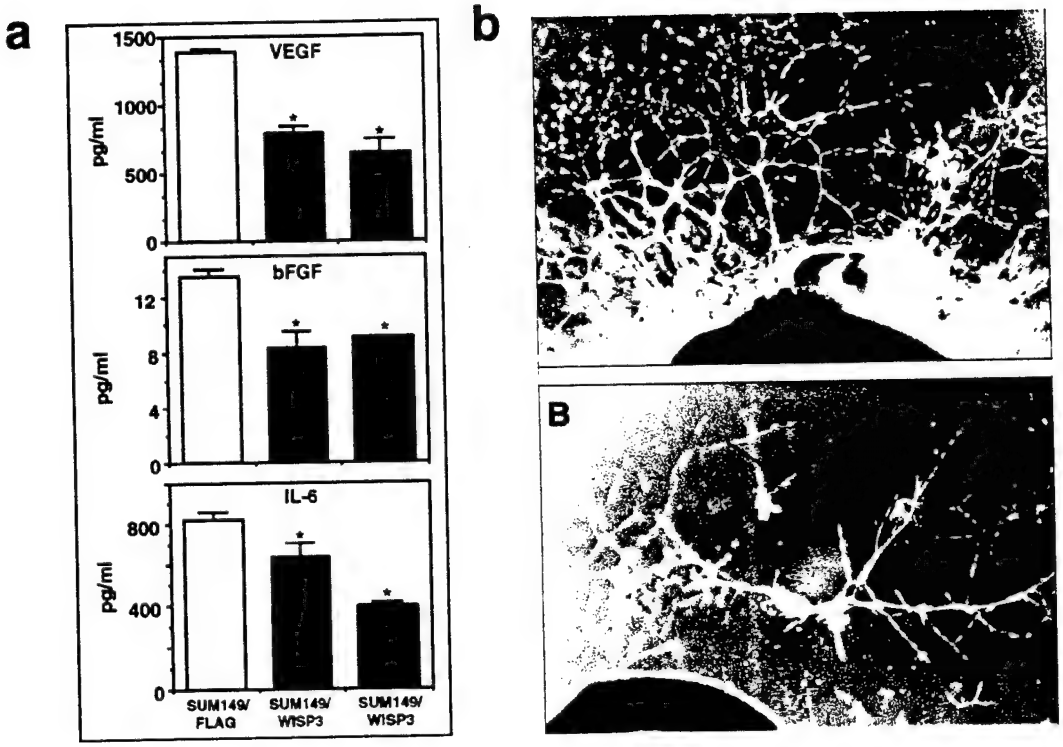
a
VEGF
1500
1000
500
0
pg/ml
bFGF
12
8
4
0
pg/ml
IL-6
800
400
0
pg/ml
SUM149/ FLAG
SUM149/ WISP3
SUM149/ WISP3
b
B

FIG. 4

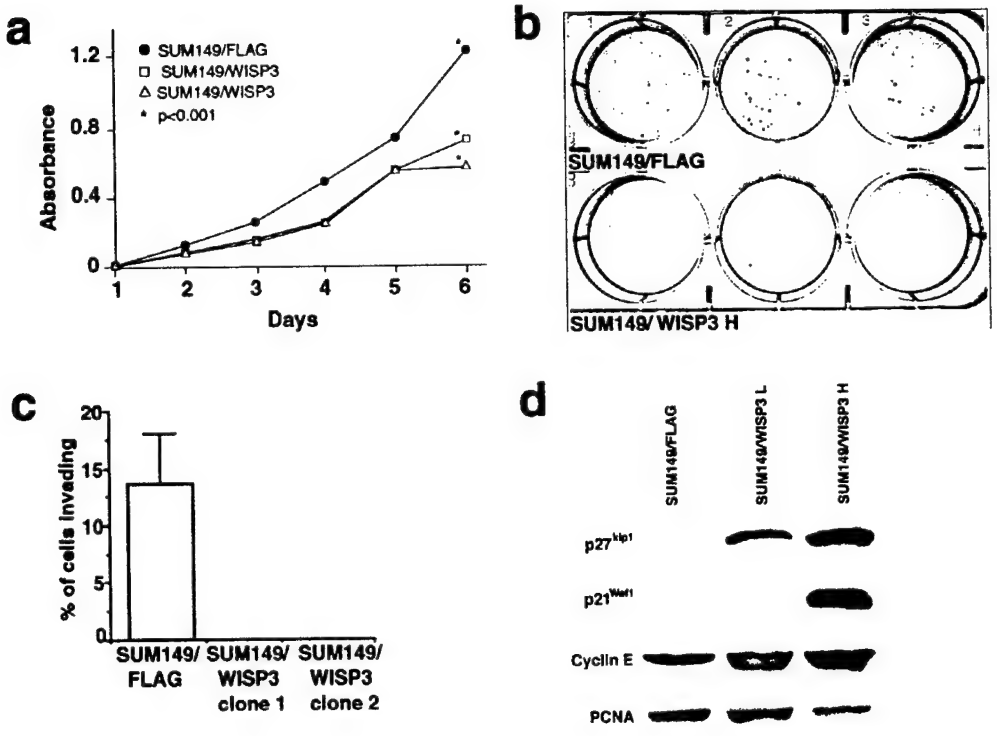
a
SUM149/FLAG
SUM149/WISP3
SUM149/WISP3
* p<0.001
Absorbance
1.2
0.8
0.4
0
1
2
3
4
5
6
Days
b
SUM149/FLAG
SUM149/ WISP3 H
c
% of cells invading
20
15
10
5
0
SUM149/ FLAG
SUM149/ WISP3 clone 1
SUM149/ WISP3 clone 2
d
SUM149/FLAG
SUM149/WISP3 L
SUM149/WISP3 H
p27Kip1
p21Waf1
Cyclin E
PCNA

FIG. 5.

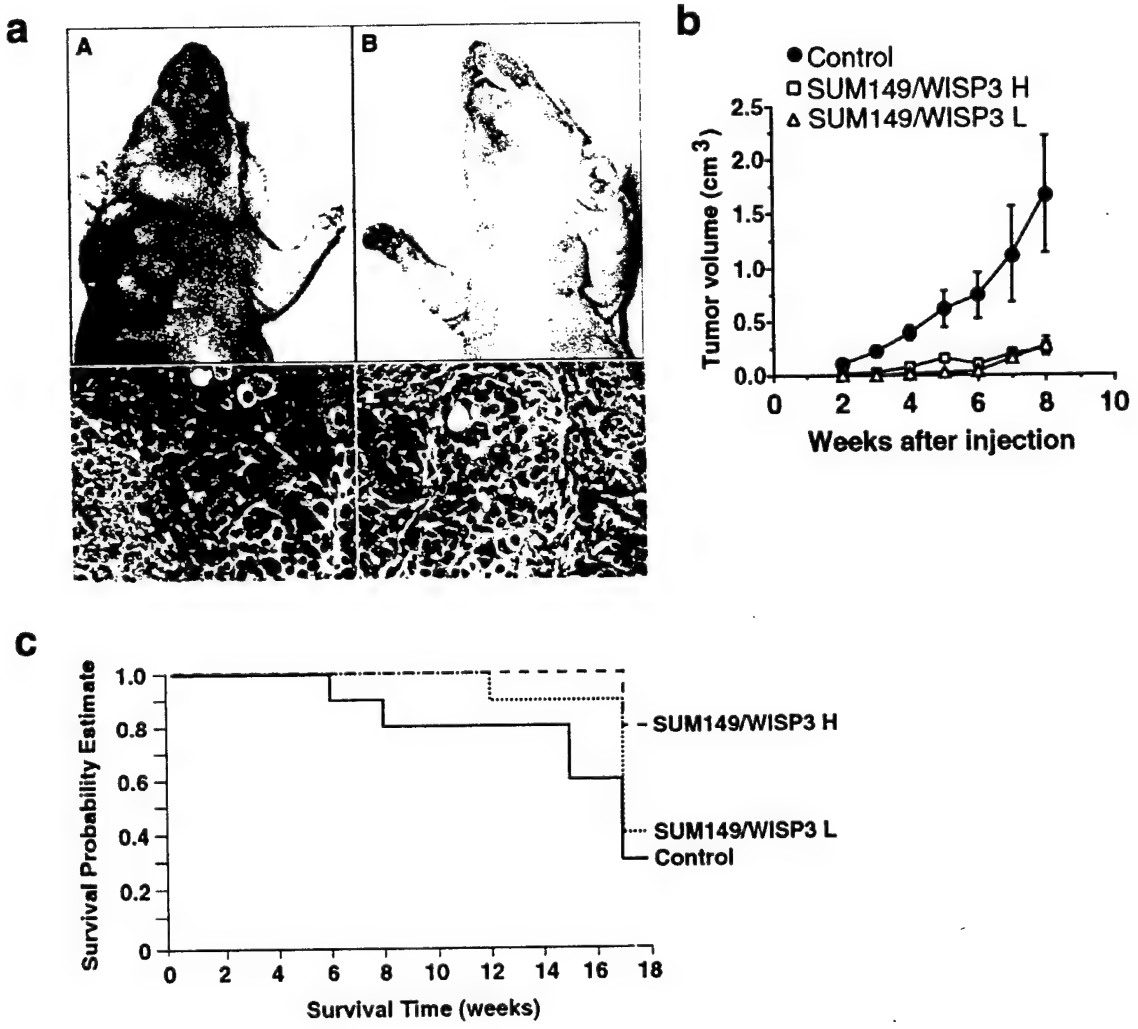
a
A
B
b
Control
SUM149/WISP3 H
SUM149/WISP3 L
Tumor volume (cm 3)
2.5
2.0
1.5
1.0
0.5
0.0
0
2
4
6
8
10
Weeks after injection
c
Survival Probability Estimate
1.0
0.8
0.6
0.4
0.2
0
0
2
4
6
8
10
12
14
16
18
Survival Time (weeks)
SUM149/WISP3 H
SUM149/WISP3 L
Control

Characterization of RhoC Expression in Benign and Malignant Breast Disease: A Potential New Marker for Small Breast Carcinomas with Metastatic Potential

Celina G. Kleer, M.D., Kenneth L. van Golen, Ph.D., Yanhong Zhang, M.D., Zhi-Fen Wu, M.D., Mark A. Rubin, M.D., and Sofia D. Merajver, M.D., Ph.D.

Departments of Pathology (CGK, MAR), Internal Medicine, Division of Hematology and Oncology (KvG, SDM, ZFW, YZ) and the University of Michigan Comprehensive Cancer Center (CGK, KvG, SDM, MAR, ZFW, YZ), Ann Arbor, Michigan.

Running Title: RhoC expression in breast

Corresponding author

Celina G. Kleer, M.D.
Department of Pathology
2G332 University Hospital
1500 E. Medical Center Drive
Ann Arbor, MI 48109-0054
kleer@umich.edu
tel. (734) 936-6776

Abstract

The most important factor in predicting outcome in patients with early breast cancer is the stage of the disease. There is no robust marker capable of identifying invasive carcinomas that despite their small size have a high metastatic potential, and that would benefit from more aggressive treatment. RhoC GTPase is a member of the Ras-superfamily that is involved in cell polarity and motility. We hypothesized RhoC expression would be a good marker to identify breast cancer patients with high risk of developing metastases and would be useful in the clinical setting. Therefore, we set out to develop a specific RhoC antibody that could be used by immunohistochemistry (IHC), and characterized RhoC protein expression in normal, benign, premalignant, and malignant breast disease, with special focus in small (<1 cm) invasive carcinomas with metastatic potential. We evaluated 127 specimens from 116 patients. RhoC specific antibody was obtained by immunizing rabbits with a highly immunogenic and unique epitope of the RhoC protein, and confirmed by Western blot. Immunohistochemistry was performed on formalin-fixed, paraffin-embedded tissues using this polyclonal antibody at 1:1500 dilution. Immunostaining intensity was graded 0-3+ (0-1+ was considered negative, and 2-3+ was considered positive). RhoC was not expressed in any of the normal (5 cases), fibrocystic changes (5), atypical hyperplasia (7), or ductal carcinoma in situ (11), but was expressed in 23 of 52 invasive ductal carcinomas, and exclusively in those that developed metastatic disease. RhoC protein expression strongly correlated with tumor stage ($p<0.001$). Of the invasive carcinomas smaller than 1 cm, RhoC protein was exclusively expressed in 4 of 5 (80%) tumors that metastasized, and in none (0 of 5) tumors that did not metastasize ($p=0.05$). Eight of 10 primary inflammatory breast cancer

(IBC) tumors expressed RhoC protein. This is the first study that characterizes the expression of RhoC in normal breast, and in breast disease. RhoC overexpression occurs once the cancer cells have acquired invasive capabilities in non-IBC invasive carcinomas. In IBC, RhoC is consistently expressed and may be an early event. RhoC appears to be a marker of metastatic potential in breast cancer in general, and in small (<1cm) tumors in particular. Although further studies are needed to confirm and expand our results, RhoC overexpression is a candidate marker capable of identifying small invasive carcinomas that have high metastatic potential, and may guide therapeutic interventions.

Introduction

Breast cancer is the most common type of life-threatening cancer, and the second most common cause of cancer related deaths of women in the Western world. The most important factor in predicting patient outcome is the stage of the disease (1-3). Although in general, the more aggressive, the more rapidly growing, and the larger the primary neoplasm, the greater the likelihood that it will metastasize or already has metastasized, this is not always the case. There are many small breast cancers with a highly aggressive behavior and discouraging outcome that remain under treated because there is no marker capable of identifying them.

RhoC GTPase is a member of the Ras-superfamily of small guanosine triphosphatases (GTPases). Activation of Rho proteins leads to assembly of the actin-myosin contractile filaments into focal adhesion complexes that lead to cell polarity and facilitate motility (4-6). In a recent study from our laboratory, we characterized RhoC as a transforming oncogene for human mammary epithelial cells, whose overexpression results in a highly motile and invasive phenotype that recapitulates the most lethal form of locally advanced breast cancer, inflammatory breast cancer.

We hypothesized that, given the known functions of the RhoC proteins, RhoC expression would be a good marker to identify breast cancer patients with highly aggressive tumors and guide therapeutic interventions before the development of metastases. Moreover, immunohistochemistry is a reproducible and technically simple procedure that would allow to test for RhoC protein expression in the clinical setting. We set out to characterize the expression of RhoC protein in normal, benign, premalignant,

and malignant breast disease, with special focus on small (<1 cm) invasive carcinomas with high metastatic potential and/or known metastases.

Materials and Methods

Tissue Specimens.

We evaluated 127 specimens from 116 patients. Breast tissues were obtained from surgical resections and biopsies from the breast and sites of distant metastases. These cases were selected from the surgical pathology files at the University of Michigan, reviewed by the study pathologist (CGK), and placed in the following pathological categories: (a) normal breast parenchyma (5 cases), (b) fibrocystic changes (5 cases), (c) fibroadenomas (3 cases), (d) atypical ductal hyperplasia (7 cases), (e) ductal carcinoma in situ (DCIS, 11 cases), (f) invasive ductal carcinoma (61 cases), (g) other types of invasive carcinoma (lobular, 13 cases; mucinous, 6 cases; medullary, 2 cases), and (h) distant metastases (14 cases). Invasive carcinomas were subdivided by stage into stages I, II, III, and IV. Patient identifiers were removed for subsequent analyses.

Development of RhoC specific antibody.

Since RhoC GTPase has high homology to other members of the Rho family, RhoA and RhoB, both at the cDNA and the protein level, most available antibodies are cross reactive with RhoA, RhoB, and RhoC. To attempt to develop an antibody specific for RhoC and not for other Rho family members, a peptide representing a unique epitope was synthesized at the University of Michigan Protein Core. The C-terminal region peptide (GLVQVRKNKRRRGCPIL) was chosen due to its uniqueness and antigenic

potential. Following injection in rabbits, immune sera was obtained following standard techniques. Western blot confirmed the specificity of the antibody for RhoC (Figure 1). Specifically no cross-reaction was observed to recombinant RhoA.

Immunohistochemistry

Immunohistochemistry was performed on formalin-fixed, paraffin-embedded tissue sections that were cut 4 μm thick and stained with polyclonal anti-RhoC antibody. The antibody was tittered and used at a 1:1500 dilution for 30 minutes at room temperature, with no previous antigen retrieval. The detection reaction followed the Dako Envision+ System Peroxidase kit protocol (Dako, Carpinteria, CA). Diaminobenzidine was used as chromogen and hematoxylin was used as counter stain. As positive controls we used tumor xenografts from a cell line known to overexpress RhoC (SUM149) and from human mammary epithelial cells transfected with RhoC, and patient tumor specimens previously demonstrated to overexpress RhoC by *in situ* hybridization (7).

Interpretation of stains

Since RhoC protein interacts with the contractile cytoskeleton of the cell and is localized to the submembrane space, cytoplasmic stain was expected. Not surprisingly, myoepithelial cells and vascular smooth muscle cells were strongly positive in all cases, thus serving as consistent internal positive controls (Figure 2). The intensity of cytoplasmic staining was scored as 0-3+, by comparison to the positive internal controls. Diffuse, moderate to strong cytoplasmic staining characterized RhoC-positive cells (scores 2+ and 3+, Figures 2, 3 and 4). RhoC-negative cells were devoid of any

cytoplasmic staining or contained faint, equivocal staining (scores 0 and 1+, Figures 2 and 5).

Statistical Analysis

Fisher's exact test was used to assess differences in RhoC expression between invasive carcinoma of different stages, and between invasive carcinomas <1 cm with and without metastases. Fisher's exact test was also performed to study whether RhoC expression was significantly different in IBC primary tumors vs lymphatic emboli.

Results

RhoC is not expressed in normal breast, fibrocystic changes or preinvasive breast disease

We studied 5 cases of normal breast parenchyma and 5 cases of fibrocystic changes, obtained from reduction mammoplasties and breast biopsies. RhoC was not detectably expressed in the ductal epithelium in any cases (Figure 2A). In addition, the 3 fibroadenomas tested revealed no RhoC protein expression. No RhoC protein expression was seen in any cases of atypical ductal hyperplasia (7 cases) low grade ductal carcinoma in situ (6 cases), or high grade ductal carcinoma in situ (5 cases) (Figure 2B). All cases however had consistent and strong RhoC staining of myoepithelial cells and vascular smooth muscle which served as internal positive control (Figure 2).

RhoC is exclusively expressed in invasive carcinomas with metastases and its expression increases with primary tumor stage

Moderate and strong RhoC protein expression (scores 2+ and 3+) was detected in 23 of the 52 (44%) primary invasive ductal carcinomas (Table 1). Table 2 shows that only the invasive ductal carcinomas that developed metastases expressed RhoC protein, in contrast to none of the invasive carcinomas without metastases ($p < 0.05$). Not surprisingly, when invasive ductal carcinomas were categorized by stage, a strong correlation was found between RhoC protein expression and tumor stage. Specifically, the higher the stage, the higher the frequency of RhoC expression ($p<0.001$, Figure 3).

Eighty per cent of primary IBC expressed RhoC protein. The intralymphatic tumor emboli seen in the skin biopsies obtained form IBC patients however were negative ($p<0.001$, Figure 2F).

Regardless of the pathological tumor stage, RhoC expression was not detected in primary invasive lobular carcinoma, invasive typical medullary carcinomas, or invasive mucinous (colloid) carcinomas.

RhoC expression identifies small invasive carcinomas with high metastatic potential

When invasive ductal carcinomas were separated by primary tumor size, 10 tumors (19%) were smaller than 1 cm. Of these, 5 had no metastases, 4 metastasized to axillary lymph nodes, and 1 developed metastases to axillary lymph nodes and colon. Interestingly, RhoC was moderately (2+) expressed in 4 of 5 (80 %) tumors that metastasized and not expressed in all 5 invasive carcinomas that did not metastasize ($p=0.05$, Figures 2C and 4).

RhoC protein expression in breast cancer metastases

Of the 14 distant metastases (liver (3), cerebellum (1), bone (4), bone marrow (1), lung (2), large intestine (2), ovary (1), and uterus (1)), 7 (50%) expressed RhoC protein (Figure 2E). After these cases were categorized by histologic type, RhoC was expressed in 5 of 8 (62.5%) metastases from invasive ductal carcinomas, in 2 of 5 (40%) metastases from invasive lobular carcinomas, and it was negative in the 1 metastasis from a medullary carcinoma.

Discussion

The Rho (Ras homology) gene was first isolated from Aplysia and has been shown to be highly conserved throughout evolution. RhoC GTPase is involved in cytoskeletal reorganization; specifically in the formation of actin stress fibers and focal adhesion contacts (4-6). Our laboratory has recently demonstrated that RhoC is overexpressed in IBC tumors by in situ hybridization (7), and has shown that overexpression of RhoC induced the malignant transformation of immortalized human mammary epithelial cells (HME cells) by producing an aggressive, highly motile, and invasive phenotype that partially recapitulates the behavior of IBC in humans (8).

Based on these results, we hypothesized that expression of RhoC would identify invasive carcinomas that despite their small size have a highly invasive and metastatic potential, and thus develop into a useful screening tool to be used in the clinical arena. To test our hypothesis, we developed a specific and sensitive polyclonal antibody directed against the RhoC protein that can be used for immunohistochemistry, and set out to

characterize RhoC protein expression in a wide spectrum of breast pathology, from normal, benign lesions, pre-malignant and in-situ carcinomas, to invasive carcinomas of the breast.

From our results several important conclusions can be drawn. First, RhoC expression may not be an early event in the development of non-IBC breast cancer, but a later genetic alteration that occurs once the cancer cells have acquired invasive capabilities. We showed that RhoC is exclusively expressed in invasive carcinomas and not in normal breast, atypical intraductal hyperplasia, or ductal carcinoma in situ. In IBC, the most lethal type of locally advanced breast cancer that is highly metastatic from its inception, RhoC appears to occur early in its development since 80% of all primary IBC expressed the protein. These results support our previous observations that RhoC is consistenly overexpressed in IBC (7). Interestingly, none of the dermal lymphatic tumor emboli expressed RhoC. A possible explanation may be that endolymphatic tumor emboli are cohesive clumps of cancer cells and do not need to acquire motile capabilities until they reach the site of metastases, at which point the tumor cells extravasate and invade new tissues. This argument is supported by a previous study from our laboratory that showed that intralymphatic tumor emboli strongly express E-cadherin, an epithelial cell-cell adhesion molecule, that enables them to form tightly cohesive tumor emboli (9).

Second, RhoC appears to be a marker of metastatic potential in breast cancer. We demonstrated that the majority of invasive ductal carcinomas that developed metastases expressed RhoC (23 of 36 cases, 64%), in contrast to none of the invasive carcinomas without metastases (0 of 16 cases). These results are in concordance with previous data showing that overexpression of RhoC GTPase in immortalized human mammary

epithelial cells leads to a motile and invasive phenotype able to develop highly metastatic tumors when injected in nude mice (8). Not surprisingly, we found that RhoC GTPase expression increases with the stage of the invasive carcinoma, with 100% of stage IV cancers expressing the protein.

Third, our results suggest that RhoC protein detection by IHC may be a useful tool capable of identifying small invasive ductal carcinomas with high propensity to metastasize. Although the number of cases in our study is small, 80% of invasive carcinomas smaller than 1 cm that developed metastases expressed RhoC protein, in contrast to none of the small tumors that did not metastasize. We are currently expanding the number of cases to further define these observations. This potential use of RhoC in the clinical setting may have a profound impact in the management of breast cancer patients. Specifically, detection of RhoC expression may identify patients who will benefit from an axillary lymph node dissection given the high risk of metastases.

Although primary invasive lobular carcinomas did not express RhoC, 40% of their distant metastases expressed the protein, suggesting that RhoC expression may be involved in the metastatic process of this type of invasive carcinoma, but may be a later event than in non-IBC invasive ductal carcinomas. RhoC expression does not appear to play a role in the late stages of other uncommon forms of invasive breast cancer, including medullary and colloid (mucinous) carcinomas.

Since RhoC protein is associated with the contractile cytoskeleton of the cell, it is not surprising that it is detected by immunohistochemistry in myoepithelial cells and in the vascular smooth muscle cells. These two cell types served as consistent and strong (3+) internal positive controls for the antibody, and were detected in all cases.

Page intentionally left blank.

This study is the first examining the expression of RhoC GTPase protein in a wide spectrum of normal breast and of breast disease. It is clear from the results that RhoC is a specific marker of metastatic disease in patients with breast cancer. More importantly, although our data is preliminary, it reliably identifies a subset of patients with small primary tumors and high metastatic potential that would benefit from axillary lymph node staging and would remain otherwise unrecognized.

Acknowlegment We want to thank Elizabeth Horn for artwork.

References

1. Danforth D, Lichter AS, Lippmann ME. The diagnosis of breast cancer. In: Danforth D, Lichter AS, Lippmann ME (eds). Diagnosis and Management of Breast Cancer. Philadelphia, WB Saunders Co, 1988, pp 50-94.
2. Rosen PR, Groshen S, Saigo PE, Kinne DW, Hellman S. A long-term follow-up study of survival in stage I (T1N0M0) and stage II (T1N1M0) breast carcinoma. J Clin Oncol. 1989 Mar;7(3):355-66.
3. Haybittle JL, Blamey RW, Elston CW, Johnson J, Doyle PJ, Campbell FC, Nicholson RI, Griffiths K. A prognostic index in primary breast cancer.Br J Cancer. 1982 Mar;45(3):361-6.
4. Nobes CD and Hall A. Rho, rac, and cdc42 GTPases regulate the assembly of multimolecular focal complexes with actin stress fibers, lamellipodia and filopodia. Cell. 1995, 7;81(1):53-62.
5. Leung T, Chen XQ, Manser E, Lim L. The p160 RhoA-binding kinase ROK alpha is a member of a kinase family and is involved in the reorganization of the cytoskeleton. Mol Cell Biol. 1996 Oct;16(10):5313-27.
6. Kimura K, Ito M, Amano M, Chihara K, Fukata Y, Nakafuku M, Yamamori B, Feng J, Nakano T, Okawa K, Iwamatsu A, Kaibuchi K. Regulation of myosin phosphatase by Rho and Rho-associated kinase (Rho-kinase) Science. 1996 Jul 12;273(5272):245-8.
7. van Golen,K.L., Davies,S., Wu,Z.F., Wang,Y., Bucana,C.D., Root,H., Chandrasekharappa,S., Strawderman,M., Ethier,S.P., and Merajver,S.D. A novel putative low-affinity insulin-like growth factor-binding protein, LIBC (lost in

inflammatory breast cancer), and RhoC GTPase correlate with the inflammatory breast cancer phenotype. *Clin Cancer Res*, 1999, 5:2511-2519.

8. van Golen KL, Wu ZF, Qiao XT, Bao LW, Merajver SD. RhoC GTPase, a novel transforming oncogene for human mammary epithelial cells that partially recapitulates the inflammatory breast cancer phenotype. Cancer Res. 2000 Oct 15;60(20):5832-8.
9. Kleer CG, van Golen KL, Braun T and Merajver SD. Persistent E-cadherin expression in inflammatory breast cancer. Modern Pathology, 2001, 14(5), in Press.

Figure Legends

FIGURE 1. Development of specific RhoC antibody. A. Western immunoblot showing the specificity of the RhoC antibody for RhoC, without cross-reaction with recombinant RhoA, shown in panel B. C. Immunohistochemistry using RhoC antibody in a tumor xenograft developed by injecting human mammary epithelial cells overexpressing RhoC in the mammary fat pad of female athymic nude mice. Strong staining of the cytoplasm of the neoplastic cells. HME= human mammary epithelial cells, HME-β-gal= transfection controls, HME-RhoC= HME cells transfected with RhoC gene, SUM149= cell line derived from a patient with inflammatory breast cancer that overexpresses RhoC.

FIGURE 2. Results of RhoC protein detection by immunohistochemistry. A, Normal terminal duct lobular unit showing RhoC staining in the myoepithelial cells and vessels in contrast to the negative normal epithelial cells.B, High grade ductal carcinoma in situ with central necrosis and no RhoC expression. Note the positive staining of the surrounding blood vessels and occassional myoepithelial cell that serve as positive internal controls. C, Primary invasive ductal carcinoma that measures 0.6 cm with RhoC protein expression (2+). This carcinoma developed axillary lymph node metastases. D, Primary stage 3 invasive ductal carcinoma with strong (3+) cytoplasmic staining for RhoC protein. E, Metastatic ductal carcinoma from the breast to the iliac bone showing strong RhoC expression. F, Intralymphatic carcinomatous embolus in a dermal lymphatic vessel in a patient with the clinical and pathological features of inflammatory breast cancer with no RhoC protein expression. Note the positive staining of the endothelial cells.

FIGURE 3. Increasing RhoC expression with increasing stage of the invasive breast carcinoma.

FIGURE 4. RhoC expression identifies a group of invasive ductal carcinomas smaller than 1 cm that developed axillary lymph node and distant metastases.

Table 1. RhoC GTPase expression in normal breast and a spectrum of breast disease

Pathology	Negative score 0-1+	Positive score 2+-3+
Normal Ductal Epithelium	5/5	
Fibrocystic Changes	5/5	
Fibroadenomas	3/3	
Atypical Ductal Hyperplasia	7/7	
Ductal Carcinoma in Situ		
Low Grade	6/6	
High Grade	5/5	
Invasive Ductal Carcinoma		
Stage I	9/9	
Stage II	13/16	3/16 (19%)
Stage III (non-IBC)	5/13	8/13 (61%)
IBC		
Primary	2/10	8/10 (80 %)
Skin- Lymphatic Tumor Emboli	9/9	
Stage IV		4/4 (100%)
Metastases	3/8	5/8 (63%)
Invasive Lobular Carcinoma		
All Stages	13/13	
Metastases	3/5	2/5 (40%)
Invasive Medullary and Colloid Carcinoma		
All Stages	8/8	
Metastases	1/1	

FIGURE 1

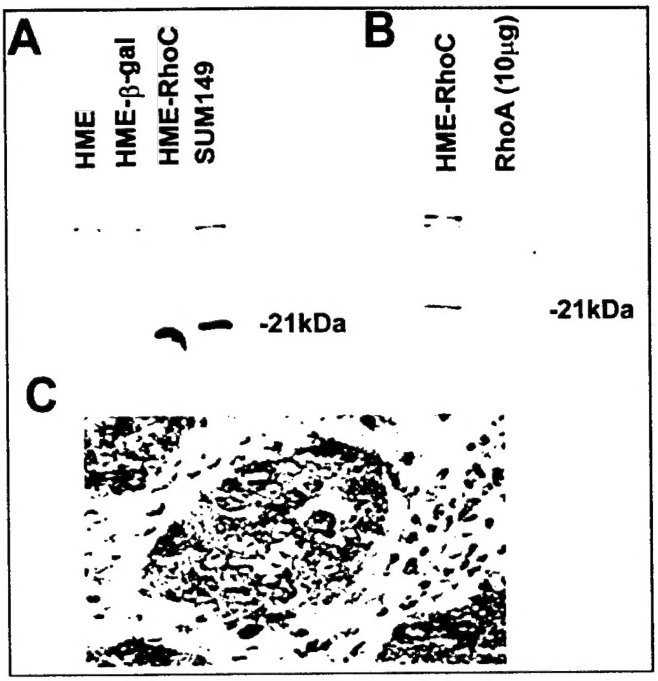
A
HME
HME-β-gal
HME-RhoC
SUM149
-21kDa
B
HME-RhoC
RhoA (10μg)
-21kDa
C

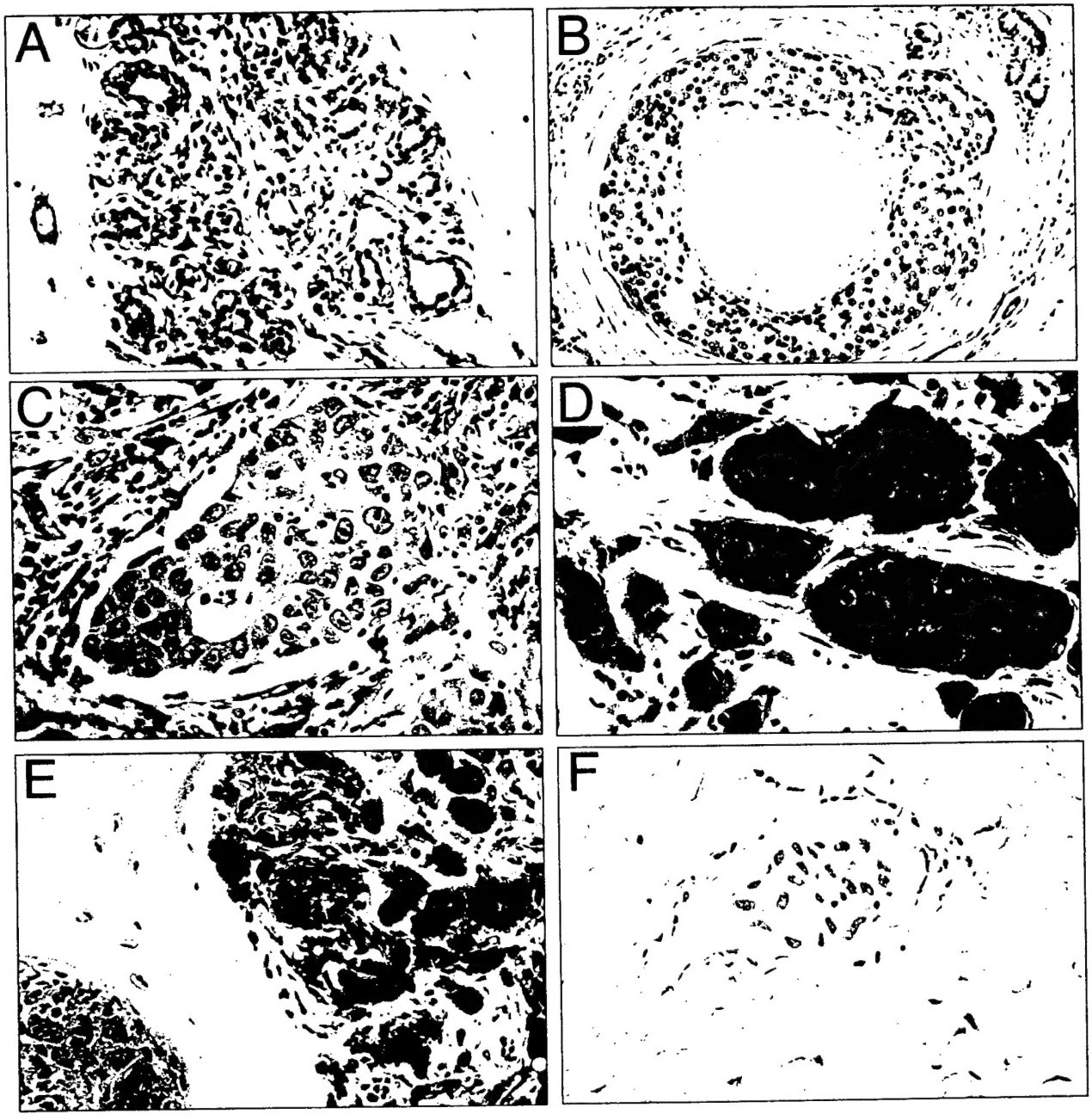
A
B
C
D
E
F

KLEER
FIGURE 3

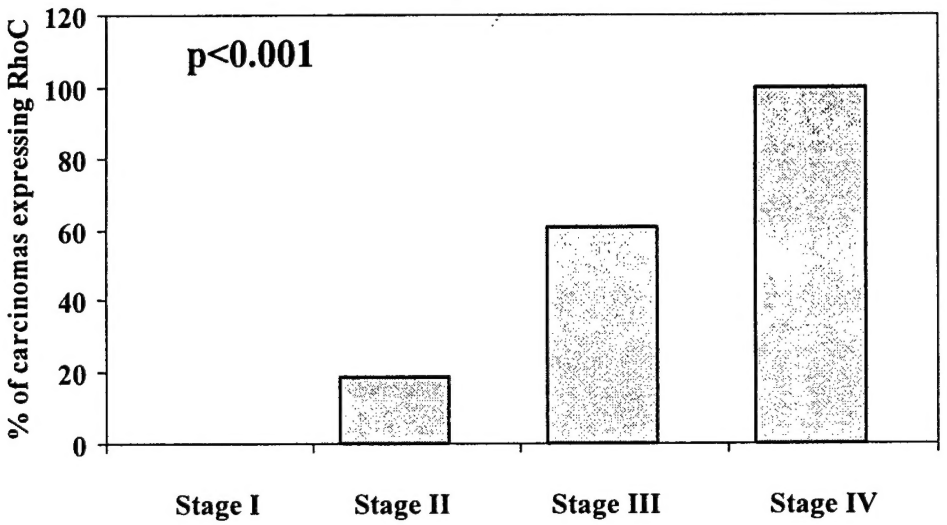

KLEE
FIGURE 4